# Politecnico di Torino

Master Degree's in Mechanical Engineering


# Numerical and experimental analysis of a heat exchanger for new generation helicopter applications

**Academic Supervisor**

Prof. Pietro Asinari

**Company Supervisor**

Lucia Azzini, PhD

Miriam Manzoni, PhD

**Candidate**

Luca Abbondanza

# Index

# Index of Figures

# Index of Tables

# List of symbols

*Latin Letters*

| | |
|---|---|
| $A$ | Area $[m^2]$ |
| $C$ | Heat capacity $\left[{}^{J}/_{K}\right]$ |
| $c_p$ | Specific Heat Capacity $\left[{}^{J}/_{kg*K}\right]$ |
| $D_i$ | Internal diameter $[m]$ |
| $\Delta T$ | Difference of temperature [K] |
| $\Delta p$ | Difference of pressure [Pa] |
| $f$ | Fouling factor [-] |
| $F$ | Correction factor for LMTD $\Delta T_{lm}$ [-] |
| $h$ | Convection heat transfer $\left[{}^{W}/_{K*m^2}\right]$ |
| $H$ | Channel height$[m]$ |
| $HTC$ | Heat Transfer Coefficient $\left[{}^{W}/_{K*m^2}\right]$ |
| $i$ | Enthalpy $\left[{}^{J}/_{Kg}\right]$ |
| $j$ | Colburn factor [-] |
| $k$ | Conductivity $\left[{}^{W}/_{m*k}\right]$ |
| $K$ | Loss coefficient [-] |
| $L$ | Length heat exchanger $[m]$ |
| $LMTD_{corr}$ | Factor correction for LMTD [-] |
| $\dot{m}$ | Mass flow $\left[{}^{kg}/_{s}\right]$ |
| $NTU$ | Number of Transfer Units [-] |
| $Nu$ | Nusselt number [-] |
| $p$ | Pressure $[Pa]$ |
| $Pr$ | Prandtl number [-] |
| $q$ | Total rate of heat transfer $\left[{}^{J}/_{s}\right]$ |
| $R$ | Thermal resistance $\left[{}^{W}/_{K*m^2}\right]$ |
| $Re$ | Reynolds number [-] |
| t | Thickness $[m]$ |

| | |
|---|---|
| $U$ | Global heat transfer coefficient $\left[{}^{W}/_{K*m^2}\right]$ |
| $W$ | Thermal power $\left[{}^{J}/_{s}\right]$ |

*Greek letters*

| | |
|---|---|
| $\alpha$ | Ratio between the width and the height of the channel [-] |
| $\delta$ | Ratio between the fin thickness and fin length [-] |
| $\varepsilon$ | Effectiveness [-] |
| $\gamma$ | Ratio between the fin thickness and width channel [-] |
| $\eta$ | Efficiency [-] |

*Subscripts*

| | |
|---|---|
| $c$ | Cold fluid |
| $f$ | Fouling |
| $in$ | Inlet section |
| $h$ | Hot fluid |
| $hx$ | Heat exchanger |
| $lm$ | Logarithmic mean |
| $out$ | Outlet section |
| $wet$ | Zone in contact with the fluid |

# Acknowledgements

First and foremost, I would like to thank GE AvioAero, which in collaboration with the Politecnico di Torino, to give me the possibility of carrying out a thesis activity in a business environment of the highest level.

A big thank acknowledgement is directed to the Aero-Thermal and Fluid System manager, Ing. Marco Del Cioppo, and to all his team. In particular, to the colleagues Lucia Azzini, PhD and Miriam Manzoni, PhD, who helped me in all activities carried out and providing me with a fundamental technical and knowledge support to accomplished the final result of the thesis.

I am also grateful to my thesis supervisor Professor Pietro Asinari for his motivation, enthusiasm and knowledge. His useful discussion and valuable suggestions have been crucial to reach the objectives of the thesis.

Furthermore, I must express my very profound gratitude to my family members for the support and continuous encouragement throughout my years of study. Heartfelt thanks to my brother Claudio for his continuous recommendations on the layout of the thesis.

This accomplishment would not have been possible without them.

Thank you.

# Abstract

The oil allows to lubricate and cool down several gearbox components that are fundamental for lift and forward flight of helicopters. The heat exchanger is the component designed to reduce the temperature of coolant fluid (oil) to preserve the functionality of helicopter gearbox components. In particular, the plate and fin heat exchanger enables rapid reduction of oil temperature by air cooling by leveraging its large heat exchange area. This type of heat exchanger are the most used in helicopter design thank to their compactness and simplicity allow to maximize thermal exchange with a lightweight configuration. However, a model to predict and characterize the performance of plate and fin heat exchanger is up to now not complete available and validated.

In this work, a model based on Effectiveness-Number Transfer Units (ε-NTU) algorithm was developed. Exploiting the approximation of average fluids thermodynamic properties for zero dimensional (0D) design, we permit to provide a fast, scalable and detailed model for a rapid design and experimental validation for air-oil, counterflow, plate and fin heat exchanger. In particular, our model allow to estimate several parameters of oil cooling system including heat load, fluids temperature and heat exchanger efficiency. To evaluate our model performance, it was validated using a several data sets both published and unpublished experimental data. Our model predicts the results with a relative deviation less than 10% compared with the experimental data.

Overall, by providing a novel set of equations for a plate and fin heat exchanger our work will allow to minimize the size of heat exchanger to achieve the maximum required heat load. This, in turn, enable to design smaller and lightweight heat exchanger with improved performances to achieve new generation helicopter gearboxes requirements.

# Chapter 1

# Introduction

Heat exchanger is used in many engineering applications ranging from heating and cooling, energy applications (power generation) to aeronautics and land vehicles. It can be said that this component is present in many devices that are used every day (for example the car). Its task is to take away the heat from the component because an excessive component temperature could leads to a failure and jeopardize the safety of the system. Indeed, in a helicopter system the heat exchanger is usually used to decrease the oil temperature to correctly lubricate and cool down the gearbox components.

The heat exchangers components manufacturing technology has been improved along the years and now allow us to manufacture extremely compact heat exchangers. In the near future, leveraging on the additive manufacturing technology, it will be possible to build even more efficient and compact heat exchangers than the current ones with special geometry not manufacturable today (Figure 1).

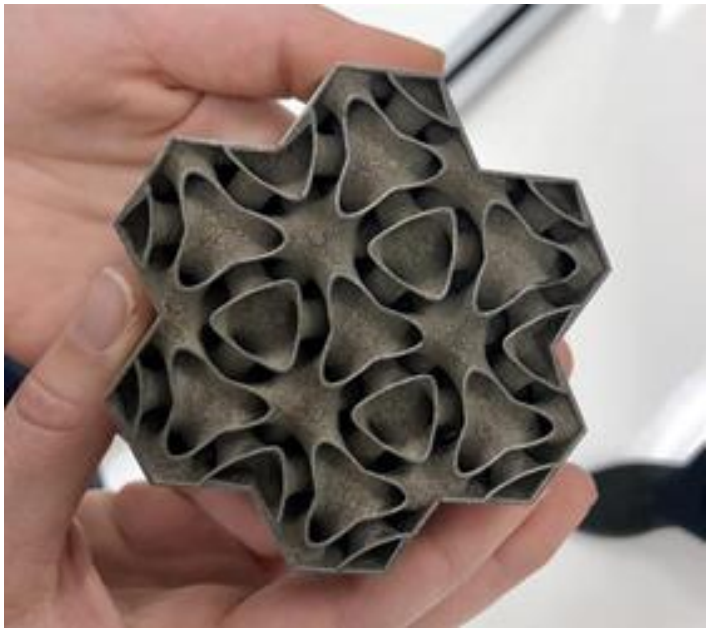

*Figure 1 – A prototype of the new heat exchanger type (GE Report)*

## 1.1. Case study

The aim of this thesis is to provide a model, which it permits to evaluate the performance of counterflow, plate and fin heat exchangers, characterized by oil and air as working fluids. Such exchangers are largely used for oil cooling in aviation, and has specific requirements, such as compactness and weight. These requirements are increasingly stringent for fuel consumption and emissions reduction. Having smaller and more efficient heat exchangers in new generation helicopters contributes to achieve these objectives.

The new targets can be achieved with innovative heat exchanger designs that require dedicated tools to obtain fast, scalable and detailed results.

The main objective of the present work is to develop and validate a model for the performance predictions of counterflow, plate and fin heat exchangers, adopting the ε-NTU method. The model provides, for a given several input including geometrical parameters, air and oil flow rate, an estimation of some parameters, including:

a) heat load
b) fluids temperatures
c) heat exchanger efficiency

to improve the prediction of oil cooling systems onboard.

*Figure 2 – One of the new helicopter designs concepts to meet the new stringent requirements*

## 1.2. Organization of the thesis

The work has been arranged into 8 chapters. Chapter 1 deals with general introduction and explain the aim of the thesis

Chapter 2 deals with general explanation of all type of heat exchanger available on the market.

Chapter 3 deals with the designs available in the literature, the definition of main parameters of the heat exchange, the correlations available in the literature.

Chapter 4 describe the tool, the hypothesis assumed, the correlation implemented and how the tool works.

Chapter 5 deals with the validation of the model, the paper used, the results obtained, and the analyses carried out on these experimental data.

Chapter 6 deals the validation with the internal experimental data

Chapter 7 and Chapter 8 deal respectively the conclusion and recommendations

# Chapter 2

# Classification of heat exchanger

The heat exchangers are classified according to flow arrangement or type of construction as shown to the scheme in Figure 1.

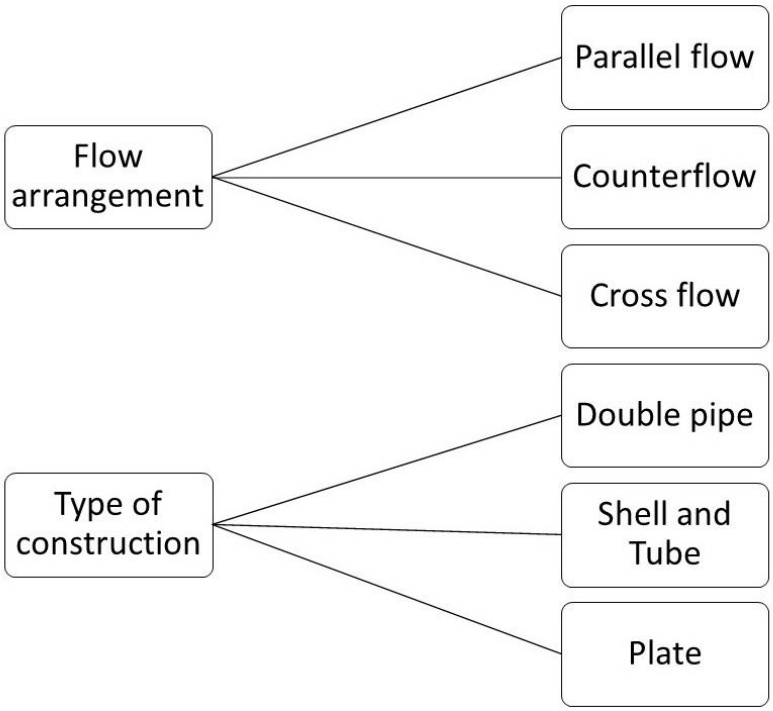


*Figure 3 - Classification of heat exchanger*

According to flow arrangement, the heat exchangers are divided in parallel flow, counterflow and cross flow and it indicates how the fluids move inside the structure.

According to type of construction, the heat exchangers are divided in large categories as double pipe, shell and tube and plate. Each category has some sub-categories that will be described in the following paragraphs.

In the following paragraphs will describe the characteristic of the different heat exchanger types available in the market. We will analyze how the heat exchanger works in relation to the flow arrangements or construction types and the properties of the construction type subcategories.

## 2.1. Flow arrangements classification

The first arrangement is the parallel flow, where the hot and cold fluids enter from the same end, flow in the same direction and exit from the same end. This type of flow is the simplest and is used in heat exchanger with concentric tube (Figure 4a). The second set-up is counterflow, where the two fluids have two opposite moving directions (Figure 4b).

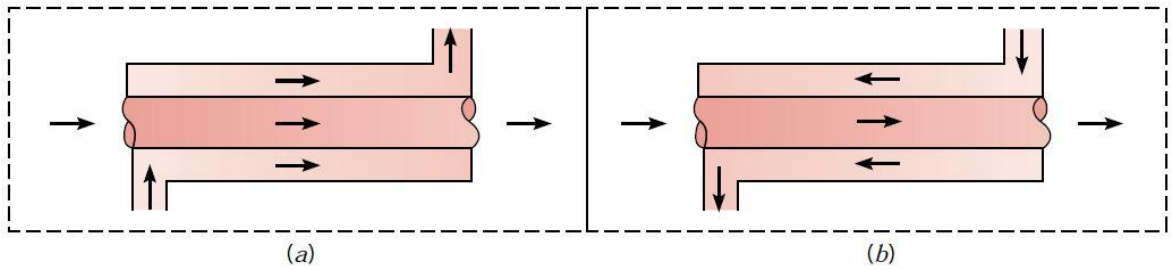


*Figure 4 - Parallel flow (a) and counterflow (b) [1]*

The third arrangement is the crossflow, where the fluids move in cross flow, i.e. along directions perpendicular to each other, as shown in Figure 5.

For the latter arrangement, it is possible to identify heat exchanger with mixed or unmixed fluids. The classification is based on the possibility of the fluids to mix or not along their path in the component. Figure 5a reports an example of an unmixed-unmixed heat exchanger, where in this set up the plate create different paths and the coolant fluid is strongly guided by walls and therefore is not able to mix tangentially. Instead, in Figure 5b is represented the same set up without plates, create a mixed-unmixed heat exchanger. In this arrangement, the coolant fluid will mix tangentially due to 3D flow phenomena influencing the heat exchanger performances.

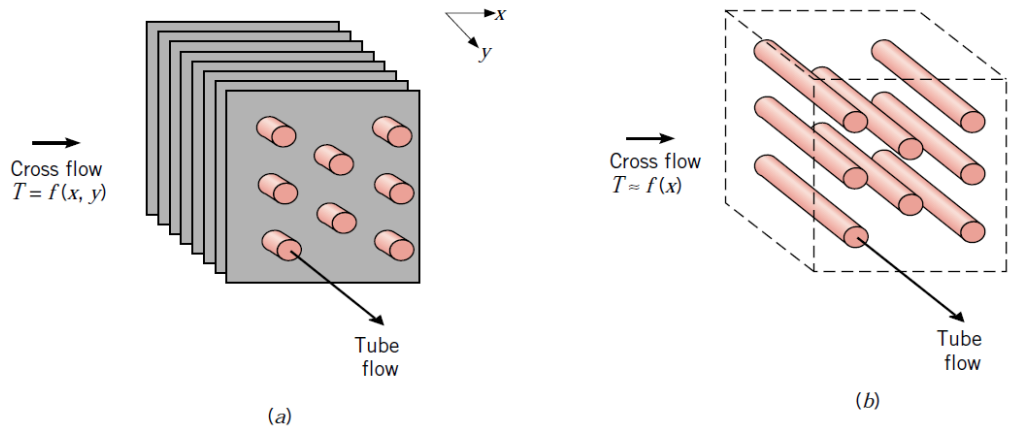


*Figure 5 - Cross-flow heat exchangers. (a) Finned with both fluids unmixed. (b) Unfinned with one fluid mixed and the other unmixed. [1]*

## 2.2. Construction Type's classification

Most of the classical configurations or industrial heat exchangers are represented in Figure 7:

a) double pipe
b) shell and tube
c) plate
d) plate and fin.

The simplest configuration is the double pipe type, characterized by two concentric tube. This configuration is cheap for both design and maintenance, making it a good choice for small industries. On the other hand, its low efficiency coupled with the high space occupied in large scales, has led to use more efficient heat exchanger type, like shell and tube or plate, because with the same thermal power exchange their size is smaller. In the next paragraphs will be described the other configurations (Figure 4) [1].

***Shell and tube***

The heat exchanger "Shell and tube" consist of a series of tubes within a box (shell). In many applications, the tubes contains the fluid that is being heated. In the shell there is the other fluid, that usually it is being cooled.

The tube bundle indicates the all tubes inside the shell and their configuration can be of several type: plain, longitudinally finned, etc. A shell and tube heat exchanger has usually used for high-pressure application because the structure of this type of heat exchanger can resist high forces on its surface without damage [1] (Figure 6).

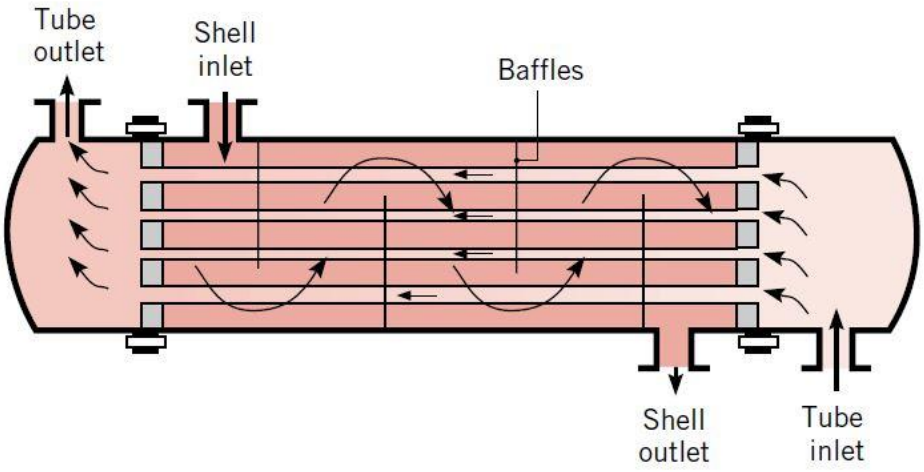


*Figure 6 - Shell-Tube heat exchanger with one shell pass and one tube pass (cross-counterflow type) [1]*

The tubes can be straight or bend to form a U shape. If it is the second heat exchanger configuration, then the fluid in the tube passes through the shell at least twice. In this configuration, the heat transfer is greater respect the one passage configuration.

For design of shell and tube heat exchanger is necessary to consider many geometrical and thermal parameters to obtain the best performance from the input of the case of interest.

The important main parameters for the design and good efficiency are:

- *Tube diameter*: If the tube diameter is small, the exchanger will be compact. In this case, the available passage section will be smaller, and the risk of fouling or clogging will be high. For this quantity, it is necessary to consider the specific application and the related problems. The tube thickness should also be taken into account in order to meet the requirements for the study application, especially if the fluid is under pressure [1].
- *Tube length*: For the less production cost, the shell and tube will be made with very long tubes and compact shells because the production of these components are uniformed. However, in all cases there are always a constraints, so it is necessary to reach a compromise between the performance and the production cost [1].
- *Tube pitch*: it is a good practice to have a tube pitch of 1.25 times the tube diameter itself. A tube pitch that is too large causes a huge shell that does not bring any benefits [1].
- *Tube Layout*: refers to how tubes are positioned within the shell and the configuration has an impact on heat exchange and its efficiency. The configuration can be: 30°, 60°, 90° or 45°. These configurations permit to obtain the best heat transfer and structural resistance [1].

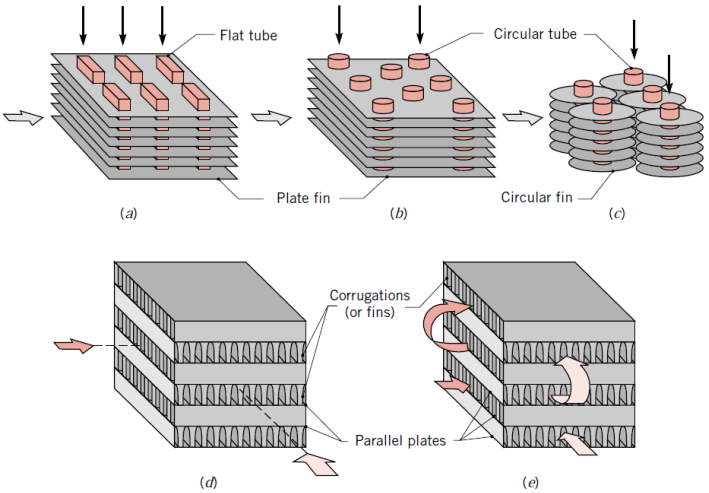


*Figure 7 - Different type of construction of compact heat exchanger* [1]

***Plate Heat Exchanger***

The Plate Heat Exchanger is a compact type of heat exchanger that uses a series of thin plates to transfer heat between two fluids. There are four main types of Plate heat exchanger: gasketed, brazed, welded, and semi-welded.

A plate heat exchanger consists of a series of plates one next to the other, where in one flows the hot fluid and in the next the cold fluid and so on. The heat flux is transferred from the hot to the cold fluid through the plates that divide them. The two fluids arrive through the two holes, made in the corners of the plates, and flow into the small channels that have formed between the plates. The plates are held together by two bars, upper and lower, and packed together thanks to the tie bolts even if the fluids are under pressure (Figure 8). This allows having a small thermal resistance for the heat flux [2].

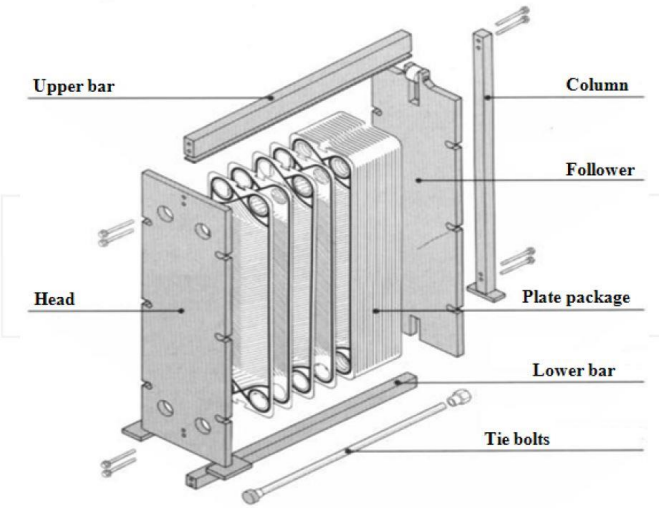


*Figure 8 – Exploded view of a plate heat exchanger* [2]

The important part of the exchanger is the plate. This structure allows to transfer the heat from the hot fluid to the cold fluid. Several plate heat exchangers design have a flat plates but for a better performance the plates can have corrugations that permits to increase the exchange area for both fluids without raise the overall size (which are shown in the Figure 9).

These corrugations are inserted on the plates to increase the heat flux, because they disturb the flow of fluid that becomes turbulent. The plates need to have a zig-zag channels, with a specific chevron angle that allows to increase the heat exchange without increasing the exchange area, i.e. it is imposed a swirling motion to the fluid (Figure 10). Multi-pass arrangements can be implemented, depending on the arrangement of the gaskets between the plates [2].

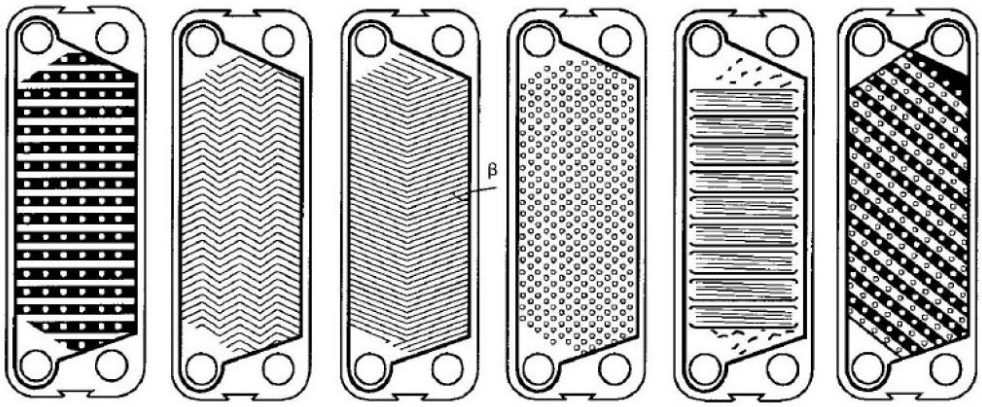


*Figure 9 - Different type of plate corrugations* [2]

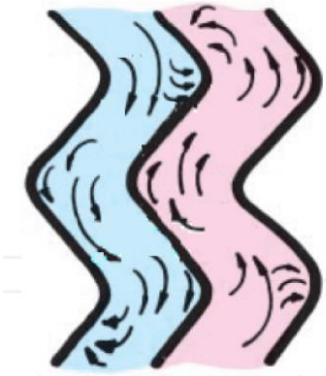

*Figure 10 - Turbulent flow in plate heat exchanger channels* [2]

The main advantages and disadvantages of a plate heat exchanger compared to shell and tube exchangers are [2]:

- *Flexibility:* Easy disassembly and cleaning of the plates from the fouling and possibility to easily adapt to different thermal power values by removing or adding plates.
- *Good temperature control*: The channels where the fluids flows are small (micro-channel) so the heat exchanger has a small transition time and has no stagnation points or overheating.
- *Efficient heat transfer*: Thanks to the small hydraulic diameter and the corrugation of the surfaces, the flow becomes easily "turbulent" and this allows an increase of the heat flux.
- *Compactness*: Thanks to its high thermal efficiency for the characteristics mentioned above, its overall dimensions are contained, which allow it to be installed even in limited spaces.
- *Reduced fouling*: This exchanger has a lower risk of fouling compared to the shell and tube type, thanks to the fact that the fluid is in a turbulent condition and the flow rates are small and ease of cleaning.

***Plate and Fin Heat Exchanger***

A plate-fin heat exchanger (PFHE) is a compact heat exchanger type that consists of flat plates and corrugated fin brazed together. Together, they form a block that can be repeated several times. The flows of the two fluids can be counterflow or crossflow. The heat transfers through the fins, thanks to the phenomenon of the convection of the fluid on the metal walls, and the phenomenon of the conductivity through the metal of the fins (Figure 11). The main aim of the fins is to help the heat to be transferred from hot to cold fluid but also provide structural support to the entire heat exchanger, in order to create channels for the two fluids. There are different fin types that allows to obtain the best performance from the case of interest [3].

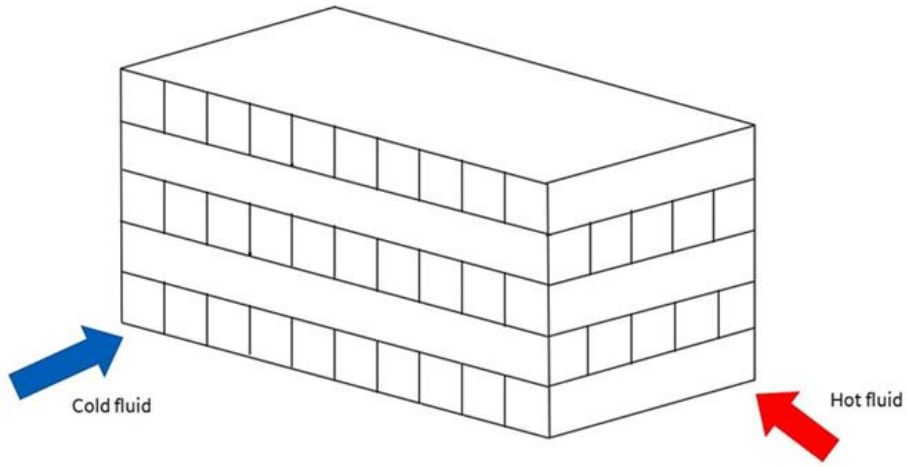


*Figure 11 - Plate and fin counterflow heat exchanger*

Available in the market several types of fin exist for different purpose but for the plate and fin heat exchanger the main fin types used are (Figure 12):

- plain, which refer to simple straight-finned triangular or rectangular designs (Figure 12b);
- herringbone or wavy, where the fins are placed sideways to provide a zig-zag path (Figure 12c);
- serrated and perforated which refer to cuts and perforations in the fins to augment flow distribution and improve heat transfer (Figure 12d).

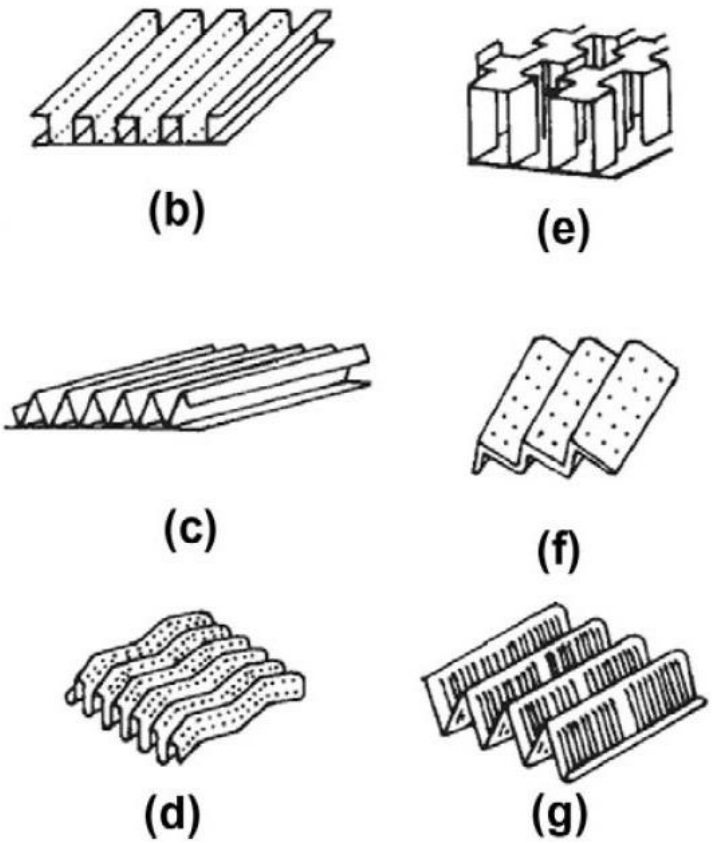


*Figure 12 - Type of fin – (b) Plain rectangular fins; (c) plain triangular fins; (d) wavy fins and herringbone fins; (e) offsets strip fins; (f) perforated fins and (g) louvered fins [4]*

- *Principal Components of a Plate Fin Heat Exchanger*

In a plate-fin heat exchanger, the heat is transferred from the hot fluid to the adjacent fins (convection on the wall), the fins transport the heat, by conduction, to the partition plate. From the plate, the heat is transferred to the fins in contact with the cold fluid (convection). The fins allow having a higher exchange surface without increasing the overall size of the heat exchanger.

This type of heat exchanger has a high degree of flexibility because it can operate with any combination of gases, liquids and two phase fluids. Compared to the types of exchangers described above, it has some important advantages:

- very close temperature approaches
- high thermal effectiveness
- large heat transfer area per unit volume
- low weight per unit transfer

Also, for this type of exchanger, in the traditional approach to design, pressure drops are considered as a constraint. The objective, during the design, is to choose a channel geometry

that allows to obtain the required thermal power, with a pressure drop that can be sustained without a failure of the entire fluid system [3].

After seen the available heat exchanger on the market and their strengths and weakness of all configurations, we will analyze in the next chapter how the thermal modelling available in the literature works and what equations it needs.

# Chapter 3

# Heat transfer modelling

To evaluate the best performance of a several heat exchangers for the case of interest, it is essential to relate the total heat transfer rate to some quantities such as the inlet and outlet fluid temperature, the overall heat transfer coefficient, and the total surface area for heat transfer. First of all, calling $q$ the total rate of heat transfer between the hot and cold fluids and assuming the system adiabatic, i.e. negligible heat transfer between the exchanger and the environment, the steady flow energy equation gives [1]:

$$q = \dot{m}_h\left(i_{h,in} - i_{h,out}\right) \tag{1}$$

and

$$q = \dot{m}_c\left(i_{c,in} - i_{c,out}\right) \tag{2}$$

where:

- $q$ is total rate of heat transfer
- $\dot{m}$ is mass flow
- $i$ is the fluid enthalpy
- $h$ and $c$ refer to the hot and cold fluids

In the simplified case in which:

i. fluids are not undergoing a phase transition
ii. fluids can be assumed as characterized by a constant specific heats ($c_p$)
iii. the contributions of kinetic and potential energy for the two fluids are assumed negligible

So the equation (1) and (2) reduced to:

$$q = \dot{m}_h c_{p,h}\left(T_{h,i} - T_{h,o}\right) \tag{3}$$

$$q = \dot{m}_c c_{p,c}\left(T_{c,i} - T_{c,o}\right) \tag{4}$$

where the temperature appearing in the expressions refer to the mean fluid temperatures at the designated locations [1].

Relations (3) and (4) involve a total of 8 variables, 4 for each fluid considered. However, these correlations do not contain information on the heat transfer area of the component.

Another useful expression is obtained by relating the total heat transfer rate $q$ to the exactly mean temperature difference ΔT and heat exchanger geometry. So, the total rate of heat transfer $q$ can be written as [1]:

$$q = UA\Delta T_{lm} \tag{5}$$

where:

- U is the global heat transfer coefficient
- A is the total heat transfer area
- $\Delta T_{lm}$ is Logarithmic mean temperature difference

In order to evaluate the performance of heat exchanger, it is necessary to use the equations (3), (4) and (5) but to using the latter equation, it need to looking for the specific expression of the logarithmic mean temperature difference for the case of interest. The expression for this calculation can be made with the Logarithmic Mean Temperature Difference (LMDT) method [1].

## 3.1. Logarithmic mean temperature difference (LMTD)

Let us consider the Parallel Flow heat exchanger for the definition of $\Delta T_m$ because this configuration is the simplest for the calculation. The typical fluid temperature distributions associated with a parallel flow heat exchanger are showing in Figure 13.

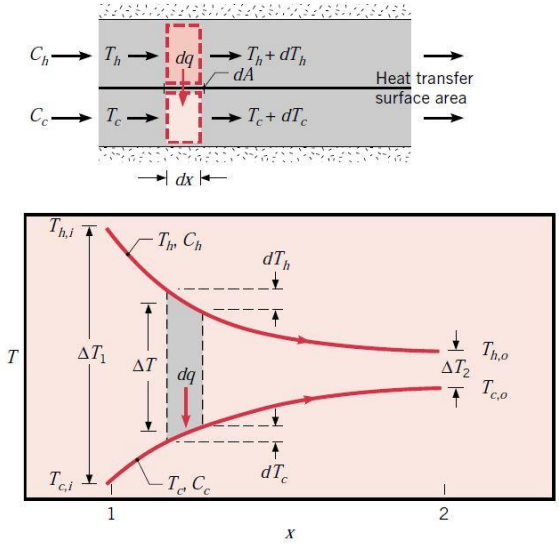


*Figure 13 - Temperature distributions for a parallel-flow heat exchanger [1]*

As can be observed, the temperature difference is initially large and decays gradually and along the heat exchanger. It is important to note that the cold fluid outlet temperature cannot be higher than the hot fluid outlet temperature. This fact limits the maximum thermal power that can be exchanged between the two fluids.

The form of $\Delta T_m$ may be determined by applying an energy balance to differential elements in the hot and cold fluids. Each element is of length *dx* and heat transfer surface area *dA*, as shown in Figure 13 [1].

The energy balances and the analysis are subject to the following assumptions:

- The heat exchanger is adiabatic, so the only transfer heat is between the hot and cold fluids
- Axial conduction along the tubes is negligible
- Potential and kinetic energy changes are negligible
- The fluid specific heats are constant along the heat exchanger
- The overall heat transfer coefficient is constant

The last two hypotheses are justified for the application considered in this thesis, as negligible variations of specific heat ($c_p$) and heat transfer coefficient (HTC) are observed along the heat exchanger. Looking of Figure 13, is possible to write [1]:

$$dq = -\dot{m}_h c_{p,h} dT_h \equiv -C_h dT_h \tag{6}$$

$$dq = \dot{m}_c c_{p,c} dT_c \equiv C_c dT_c \tag{7}$$

where $C_h$ and $C_c$ are the hot and cold fluid heat capacity.

The heat transfer across the surface area *dA* may also be expressed as:

$$dq = U\Delta T dA \tag{8}$$

where the $\Delta T$ is the local temperature difference between the hot and cold fluids in *dx* element and U is the overall heat transfer coefficient, representative of the total thermal resistance of the system.

To determine the integral form of equation (8), equations (6) and (7) can be substituting into the differential form of the temperature difference [1]:

$$d(\Delta T) = dT_h - dT_c \tag{9}$$

to obtain:

$$d(\Delta T) = -dq\left(\frac{1}{C_h} + \frac{1}{C_c}\right) \tag{10}$$

Substituting for $dq$ from Equation (8) and integrated across the heat exchanger, we obtain:

$$\int_1^2 \frac{d(\Delta T)}{\Delta T} = -U\left(\frac{1}{C_h} + \frac{1}{C_c}\right)\int_1^2 dA \tag{11}$$

and solving the integral, to obtain:

$$\ln\left(\frac{\Delta T_2}{\Delta T_1}\right) = -UA\left(\frac{1}{C_h} + \frac{1}{C_c}\right) \tag{12}$$

Substituting for $C_h$ and $C_c$ from Equation (6) and (7) respectively, it follows that:

$$\ln\left(\frac{\Delta T_2}{\Delta T_1}\right) = -UA\left(\frac{T_{h,i} - T_{h,o}}{q} + \frac{T_{c,o} - T_{c,i}}{q}\right) = -\frac{UA}{q}\left[\left(T_{h,i} - T_{c,i}\right) - \left(T_{h,o} - T_{c,o}\right)\right] \tag{13}$$

Recognizing that, for the parallel-flow heat exchanger the expressions of $\Delta T_1$ and $\Delta T_2$ are the following [1]:

$$\Delta T_1 \equiv T_{h,1} - T_{c,1} = T_{h,i} - T_{c,i} \tag{14}$$

$$\Delta T_2 \equiv T_{h,2} - T_{c,2} = T_{h,o} - T_{c,o} \tag{15}$$

then it can obtain:

$$q = UA\frac{\Delta T_2 - \Delta T_1}{\ln(\Delta T_2/\Delta T_1)} \tag{16}$$

where, it can be possible to define the logarithmic mean temperature difference (LMTD) $\Delta T_{lm}$, as:

$$\Delta T_{lm} = \frac{\Delta T_2 - \Delta T_1}{\ln(\Delta T_2/\Delta T_1)} \tag{17}$$

So, substituting the equation (17) in equation (16), we obtain:

$$q = UA\Delta T_{lm} \tag{18}$$

It is the same expression as the (5).

The same expression (17) can be obtained for counterflow heat exchanger and the expression of $\Delta T_1$ and $\Delta T_2$ are the following [1]:

$$\Delta T_1 \equiv T_{h,1} - T_{c,1} = T_{h,i} - T_{c,o} \tag{19}$$

$$\Delta T_2 \equiv T_{h,2} - T_{c,2} = T_{h,o} - T_{c,i} \tag{20}$$

Figure 14 shows a scheme for the latter configuration (counterflow).

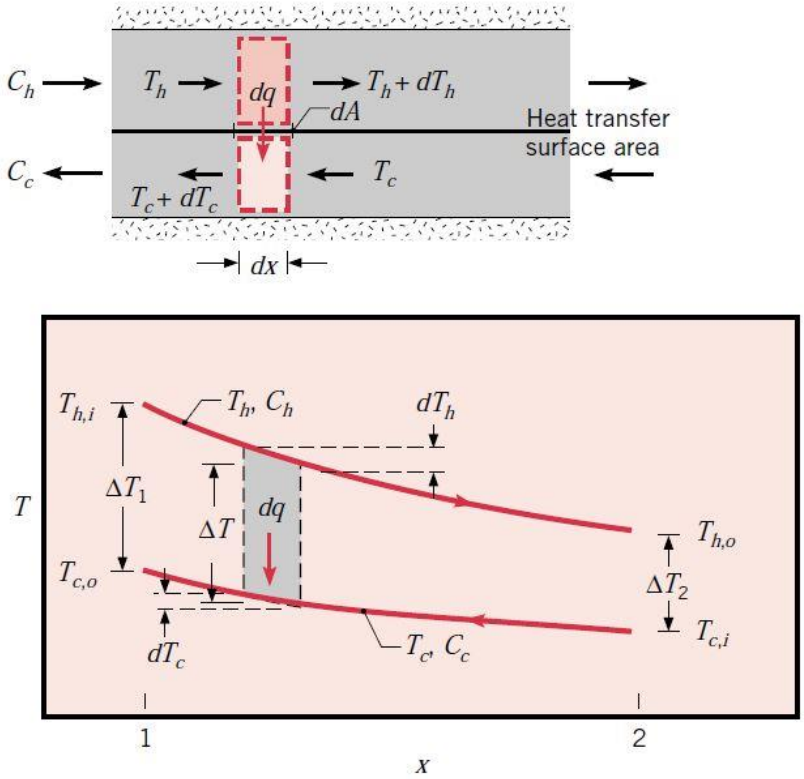


*Figure 14 - Temperature distributions for a counterflow heat exchanger [1]*

For the same inlet and outlet temperature, the value of LMTD for counterflow case exceeds that for parallel flow case. Assuming the same value of U and the same heat transfer rate $q$, the counterflow arrangement gives a smaller surface area than the parallel flow arrangement. This means being able to build a compact heat exchanger with the same thermal power output. Additionally, $T_{h,o}$ can be lower the $T_{c,o}$, increasing the thermal power exchangeable [1].

## 3.2. LMTD method for complex configurations

Equation (16) may still be used for multipass and crossflow configuration (complex configurations), by writing:

$$\Delta T_{lm} = F \Delta T_{lm,CF} \tag{21}$$

where F is a correction factor for $\Delta T_{lm}$ that would be computed under the assumption of counterflow conditions [1].

Algebraic expressions for the correction factor $F$ have been developed for various shell and tube and cross-flow heat exchanger configuration and the results may be represented graphically in the following figures. The notation (T,t) is used to specify the fluid temperature, with the variable $t$ always assigned to the tube-side fluid [1].

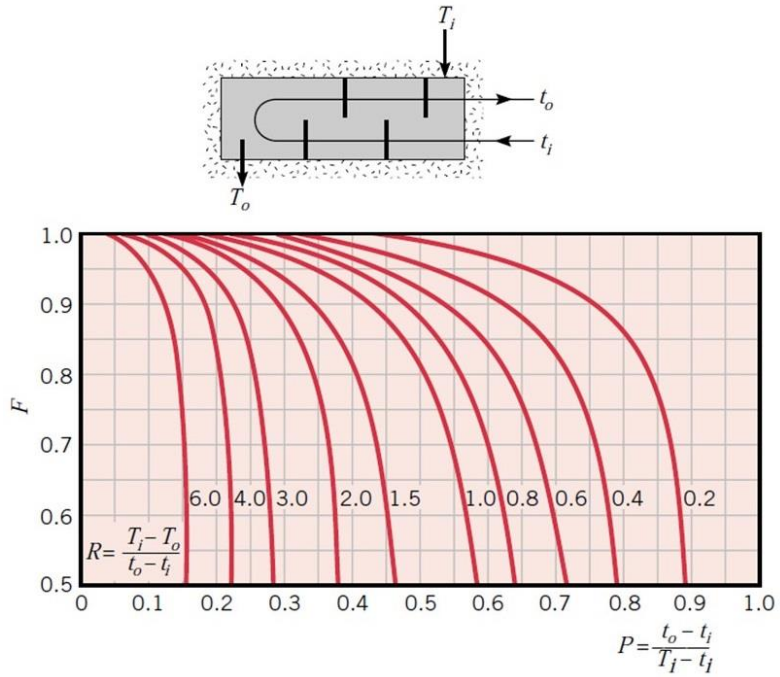


*Figure 15 - Correction factor for a shell and tube heat exchanger with one shell and any multiple of two tube passes [1]*

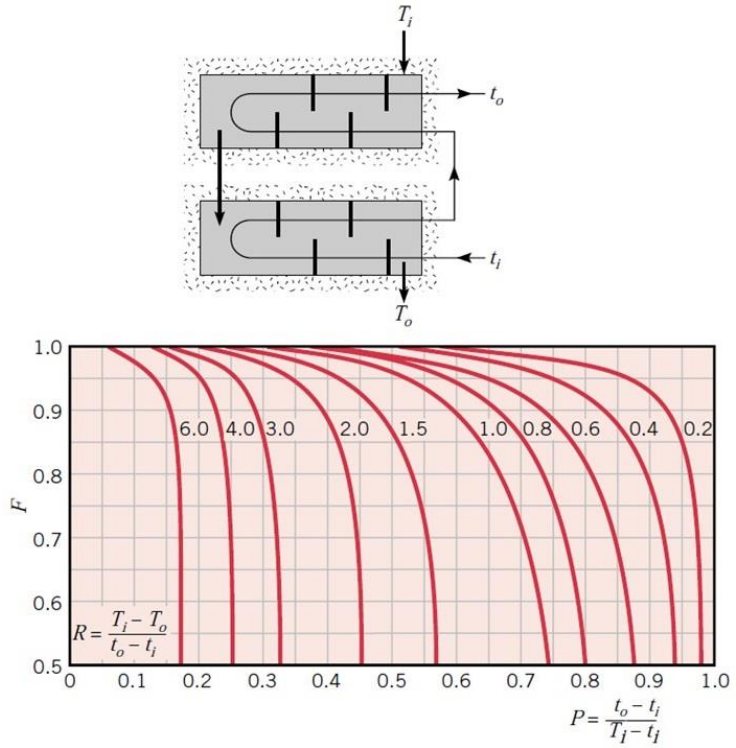


*Figure 16 – Correction factor for a shell and tube heat exchanger with two shell passes and any multiple of four tube passes [1]*

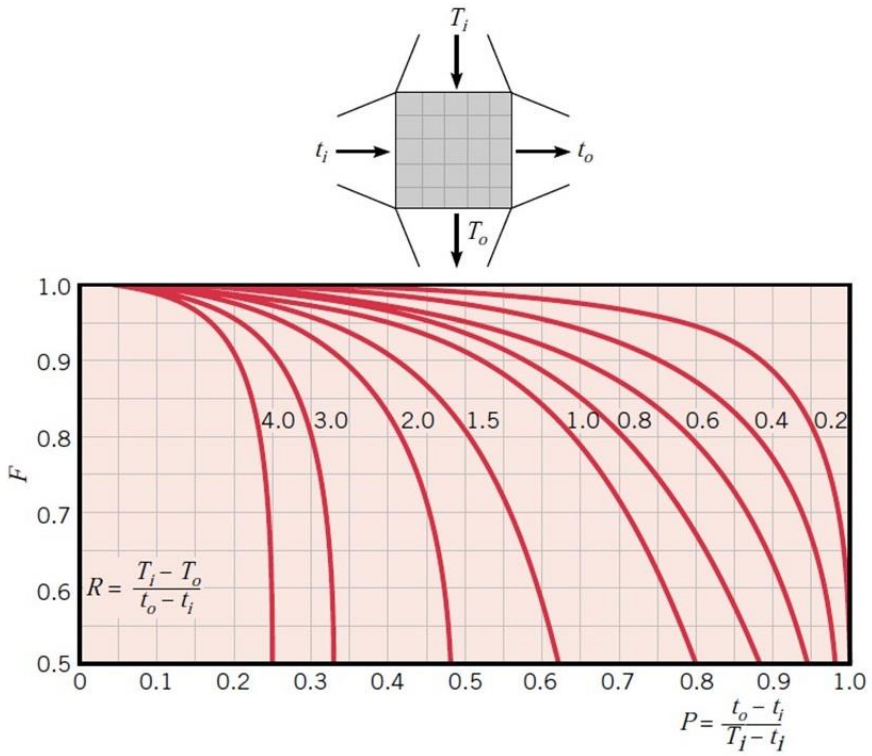


*Figure 17 – Correction factor for a single pass, cross flow heat exchanger with both fluids unmixed [1]*

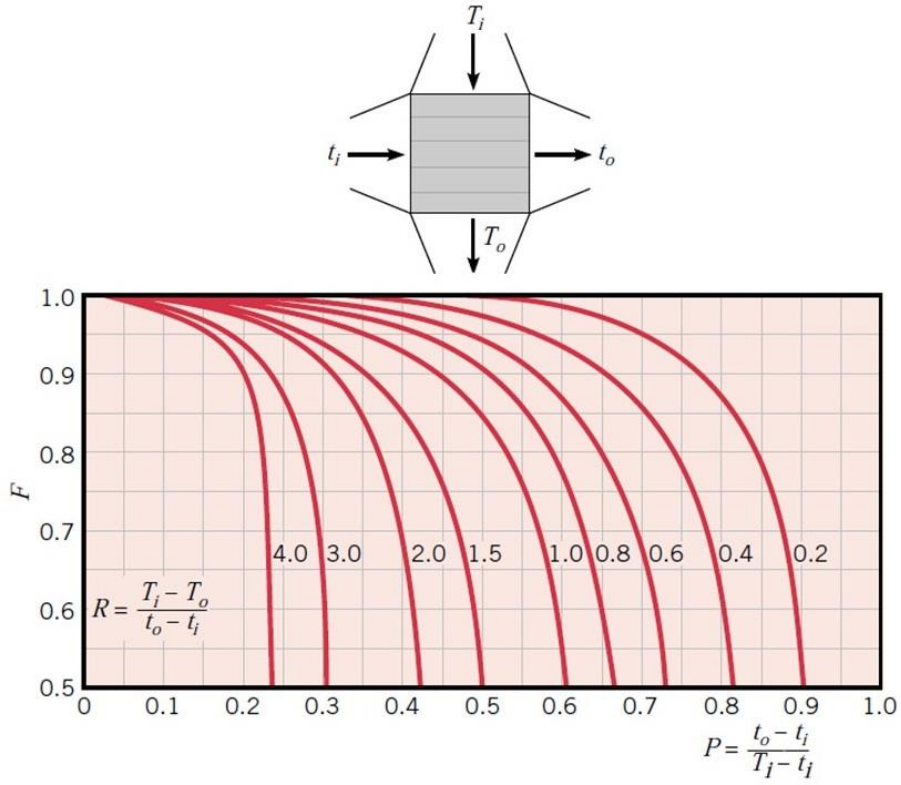


*Figure 18 – Correction factor for a single pass, cross flow heat exchanger with one fluid mixed and the other unmixed [1]*

## 3.3. Application: LMTD method for Heat exchanger design

Suppose to have a simple counterflow, concentric tube heat exchanger. Inlet temperature of hot and cold fluids, fluid flow rates and thermodynamic proprieties are known. The objective is to calculate the overall length of the heat exchanger required to exchange a given power requirement $q$.

**Procedure:**

The required heat transfer rate may be obtained from the overall energy balance for the hot fluid, equation (3). Applying Equation (4), the outlet temperatures of both fluids are:

$$T_{c,o} = \frac{q}{\dot{m}_c c_{p,c}} + T_{c,i}$$

$$T_{h,o} = -\frac{q}{\dot{m}_h c_{p,h}} + T_{h,i}$$

The heat transfer area is: $A = \pi D_i L$, where the $D_i$ is the diameter of inner tube and L is the length of the heat exchanger. Following the equation (17), the value of $\Delta T_{lm}$ can be calculated. If the metal conductivity is neglected, the global heat transfer coefficient is equal to:

$$U = \frac{1}{(1/h_c) + (1/h_h)}$$

where $h_c$ and $h_h$ is the heat transfer coefficient for the cold and hot fluids, respectively.

Now, the required heat exchanger length may now be obtained from equation (18) as:

$$L = \frac{q}{\mathrm{U}\pi D_i \Delta T_{lm}}$$

## 3.4. The Effectiveness-NTU method (ε–NTU)

The LMTD method is as fast implementation for heat exchanger analysis, when the fluid inlet temperatures are known and the outlet temperatures are specified or determined from the energy balance expressions. In addition to LMTD method, another method has been developed in literature for general cases and in case some fluid temperatures are unknown. This method is Effectiveness-Number Transfer Unit (ε-NTU).

As first, it is necessary to introduce the effectiveness parameter. The effectiveness of a heat exchanger is defined as: [1]

$$\varepsilon = \frac{q}{q_{max}} \tag{22}$$

where $q$ is the heat power of one of the fluid (equations (3) and (4)) and the $q_{max}$ is the maximum available heat power that can be exchanged, defined as:

$$q_{max} = C_{min}\left(T_{h,\mathrm{i}} - T_{c,i}\right) \tag{23}$$

where $C_{min}$ is the smaller heat capacity between the hot and cold heat capacity, $T_{h,i}$ is the inlet temperature of hot fluid and $T_{c,i}$ is the inlet temperature of cold fluid.

The effectiveness, which is dimensionless, had to be in this range $0 \leq \varepsilon \leq 1$. Having as input the parameters ε, $T_{h,i,}$ and $T_{c,i}$, the actual heat transfer rate may readily be determined from the following expression [1]:

$$q = \varepsilon C_{min}\left(T_{h,\mathrm{i}} - T_{c,i}\right) \tag{24}$$

For any heat exchangers, it can be shown that the effectiveness is function of two parameters:

$$\varepsilon = f\left(NTU, \frac{C_{min}}{C_{max}}\right) \tag{25}$$

where the Number of Transfer Units (NTU) is a dimensionless parameter that is widely used for heat exchanger analysis and it is defined as:

$$NTU = {}^{UA}/_{C_{min}} \tag{26}$$

Instead, the parameter ${}^{C_{min}}/_{C_{max}}$ can be equal to ${}^{C_c}/_{C_h}$ or ${}^{C_h}/_{C_c}$ depending on the relative magnitudes of the hot and cold fluid heat capacity rates [1].

## 3.5. The ε-NTU Relations

Suppose to consider a parallel flow heat exchanger, which is the simplest configuration available, and suppose to have $C_{min}$=$C_h$. With this hypothesis and this type of heat exchanger, it can obtain the following expression for the effectiveness [1]:

$$\varepsilon = \frac{T_{h,\mathrm{i}} - T_{h,\mathrm{o}}}{T_{h,\mathrm{i}} - T_{c,i}} \tag{27}$$

and it is possible to write:

$$\frac{C_{min}}{C_{max}} = \frac{\dot{m}_h c_{p,h}}{\dot{m}_c c_{p,c}} = \frac{T_{c,\mathrm{o}} - T_{c,\mathrm{i}}}{T_{h,\mathrm{i}} - T_{h,\mathrm{o}}} \tag{28}$$

Now consider the equation (12), which may be expressed as:

$$\ln\left(\frac{T_{h,\mathrm{o}} - T_{c,\mathrm{o}}}{T_{h,\mathrm{i}} - T_{c,i}}\right) = -\frac{UA}{C_{min}}\left(1 + \frac{C_{min}}{C_{max}}\right) \tag{29}$$

using the definition of NTU, one can obtain:

$$\frac{T_{h,\mathrm{o}} - T_{c,\mathrm{o}}}{T_{h,\mathrm{i}} - T_{c,i}} = exp\left[-NTU\left(1 + \frac{C_{min}}{C_{max}}\right)\right] \tag{30}$$

Rearranging the left-hand side of equation (30) and substituting $T_{c,\mathrm{o}}$ from equation (28), it follows that:

$$\frac{T_{h,\mathrm{o}} - T_{c,\mathrm{o}}}{T_{h,\mathrm{i}} - T_{c,i}} = \frac{\left(T_{h,\mathrm{o}} - T_{h,\mathrm{i}}\right) + \left(T_{h,\mathrm{i}} - T_{c,\mathrm{i}}\right) - \left(C_{min}/C_{max}\right)\left(T_{h,\mathrm{i}} - T_{h,\mathrm{o}}\right)}{T_{h,\mathrm{i}} - T_{c,i}} \tag{31}$$

thus:

$$\frac{T_{h,\mathrm{o}} - T_{c,\mathrm{o}}}{T_{h,\mathrm{i}} - T_{c,i}} = -\varepsilon + 1 - \left(\frac{C_{min}}{C_{max}}\right)\varepsilon = 1 - \varepsilon\left(1 + \frac{C_{min}}{C_{max}}\right) \tag{32}$$

Finally, by substituting the equation (32) into the equation (30) it follows that:

$$\varepsilon = \frac{1 - exp\{-NTU[1 + (C_{min}/C_{max})]\}}{1 + (C_{min}/C_{max})} \tag{33}$$

Same result can be obtained for $C_{min} = C_c$.

Similar expressions have been developed for a variety of heat exchangers and representative results are summarized in Table 1. In the Table 1, the parameter $C$ is the heat capacity ratio between the two fluids ($C = C_{min}/C_{max}$) [1].

| **Flow arrangement** | **Relation** | | |
|---|---|---|---|
| **Concentric tube** | | | |
| Parallel flow | $\varepsilon = \frac{1 - exp[-NTU(1+C)]}{1+C}$ | | |
| Counterflow | $\varepsilon = \frac{1 - exp[-NTU(1-C)]}{1 - C * exp[-NTU(1-C)]}$ | (C<1) | (34) |
| | $\varepsilon = \frac{NTU}{1+NTU}$ | (C=1) | (35) |
| **Shell and Tube** | | | |
| One shell pass (2,4,…tube passes) | $\varepsilon_1 = 2\left\{1 + C + \sqrt{1+C^2} * \frac{1 + exp\left[-NTU\sqrt{1+C^2}\right]}{1 - exp\left[-NTU\sqrt{1+C^2}\right]}\right\}^{-1}$ | | (36) |
| n Shell passes (2n,4n,… tube passes) | $\varepsilon = \left[\left(\frac{1-\varepsilon_1 C}{1-\varepsilon_1}\right)^n - 1\right]\left[\left(\frac{1-\varepsilon_1 C}{1-\varepsilon_1}\right)^n - C\right]^{-1}$ | | (37) |
| **Cross-flow (single pass)** | | | |
| Both fluids unmixed | $\varepsilon = 1 - exp\left[\frac{NTU^{0.22}}{C}\{exp[-C(NTU)^{0.78}] - 1\}\right]$ | | |
| $C_{max}$ (mixed), $C_{min}$ (unmixed) | $\varepsilon = \left(\frac{1}{C}\right)(1 - exp\{-C[1 - exp(-NTU)]\})$ | | |
| $C_{min}$(mixed), $C_{max}$ (unmixed) | $\varepsilon = 1 - exp\left\{\left(-\frac{1}{C}\right)[1 - exp(-C * NTU)]\right\}$ | | |
| **All exchanger (C=0)** | $\varepsilon = 1 - exp(-NTU)$ | | |

*Table 1 - Heat Exchanger Effectiveness Relations [1]*

For a shell-tube heat exchanger with multiple shell passes, it is assumed that the total NTU is equally distributed between shell passes of the same arrangement. To determine ε total, first the NTU of single shell would be calculated from Equation (36), and ε total would finally be calculated from Equation (37).

Note that for C=0, as in a boiler or condenser, the expression of ε is the same for all flow arrangement. Hence for this special case, the heat exchanger behavior is independent of flow arrangement and type of construction [1].

The foregoing expressions are represented graphically in the following figures:

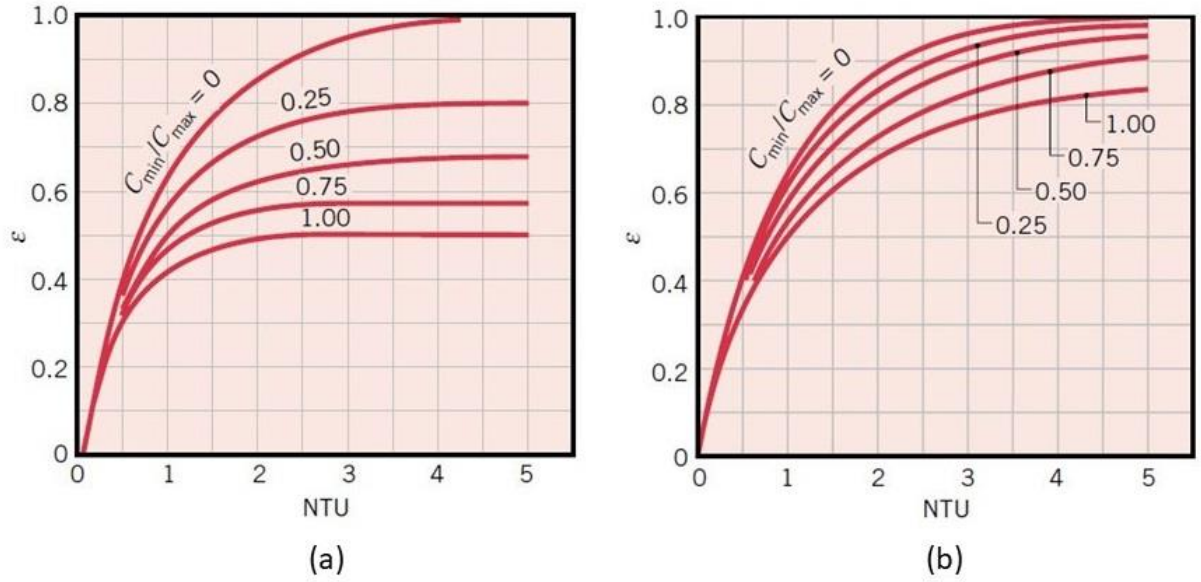


*Figure 19 - ε of parallel flow (a) and ε of counterflow (b) [1]*

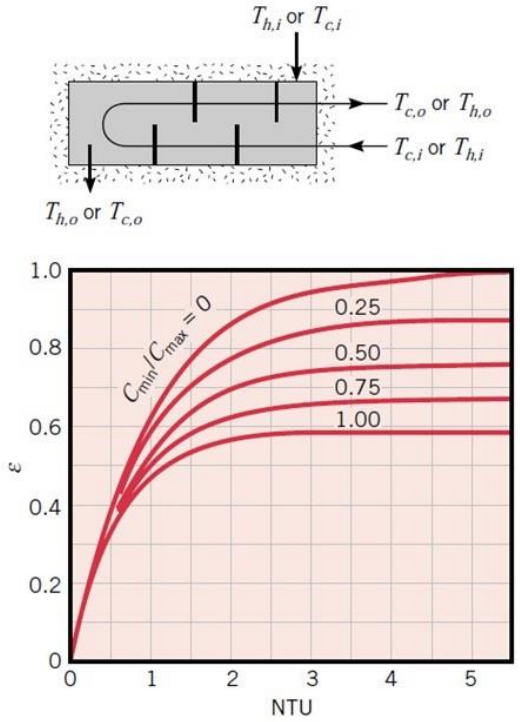


*Figure 20 - ε of a shell and tube heat exchanger with one shell and any multiple of two tube passes [1]*

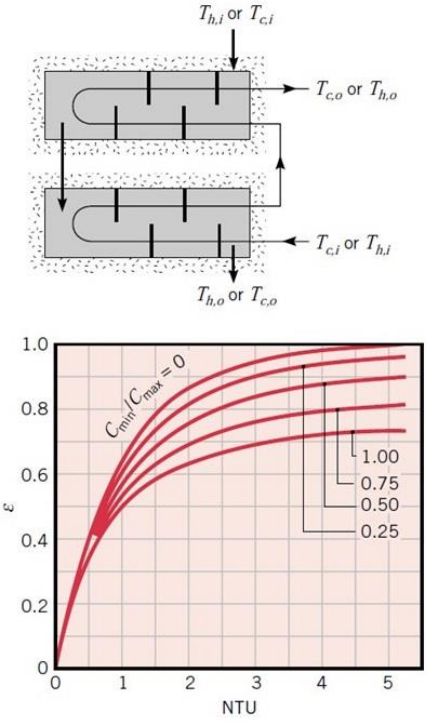


*Figure 21 - ε of shell and tube heat exchanger with two shell passes and any multiple of four tube passes [1]*

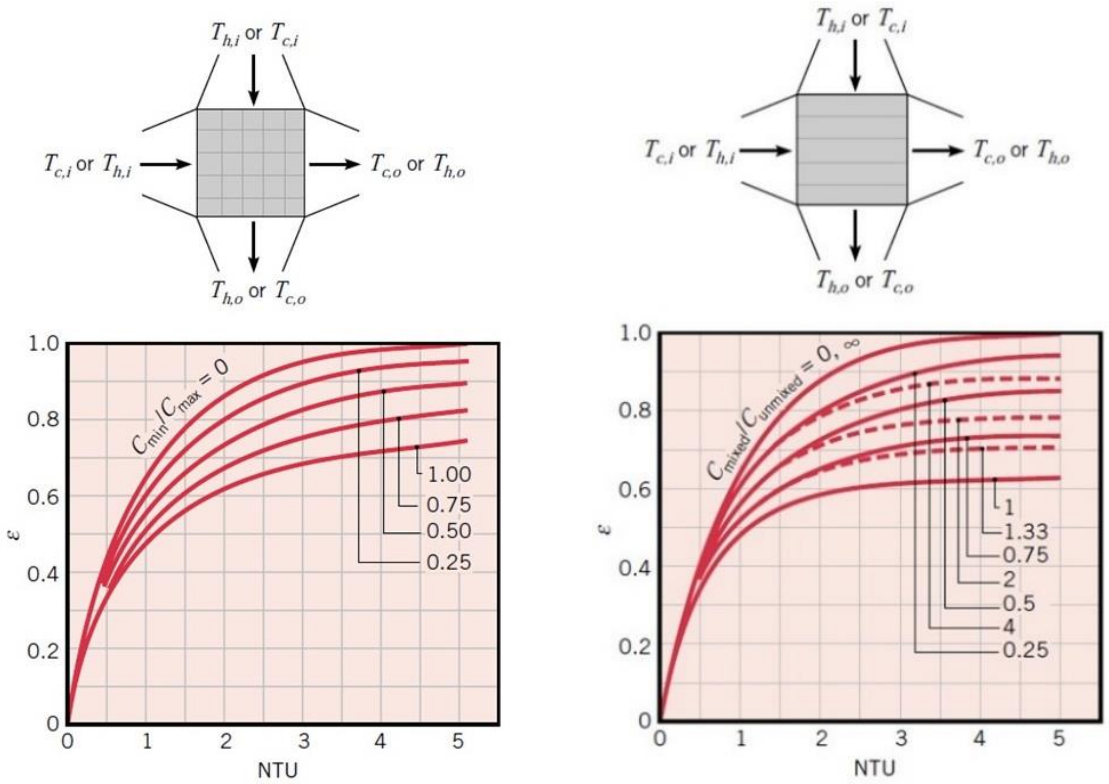


*Figure 22 - ε of a single pass, cross-flow heat exchanger with both fluids unmixed [1]*

*Figure 23 - ε of a single pass, cross-flow heat exchanger with one fluid mixed and the other unmixed [1]*

In the Figure 23 the solid curves correspond to $C_{min}$ mixed and $C_{max}$ unmixed, while the dashed curves correspond to $C_{min}$ unmixed and $C_{max}$ mixed.

It is noted that for both methods (LMTD and ε-NTU), the analysis is carried out globally on the heat exchanger and it is not investigated what happens inside it [1].

## 3.6. Application: ε-NTU method for Heat exchanger design

Suppose to have a simple counterflow, concentric tube heat exchanger. Inlet temperature of hot and cold fluids, fluid flow rates and thermodynamic proprieties are known. The objective is to calculate the overall length of the heat exchanger required to exchange a given power requirement $q$.

**Procedure:**

The required effectiveness is directly obtained from the equation (22).

The heat transfer area is: $A = \pi D_i L$, where the $D_i$ is the diameter of inner tube and L is the length of the heat exchanger. Following the equation (34) or (35), depending on the value of the thermal capacities ratio, it is possible to obtain the value of NTU.

If the metal conductivity is neglected, the global heat transfer coefficient is equal to:

$$U = \frac{1}{(1/h_c) + (1/h_h)}$$

where $h_c$ and $h_h$ is the heat transfer coefficient for the cold and hot fluids, respectively.
Now, the required heat exchanger length may now be obtained from equation as:

$$L = \frac{NTU * C_{min}}{\mathrm{U}\pi D_i}$$

After seen the two possible methods available in the literature to evaluate the performance of heat exchanger, it is necessary to explained how calculate several parameters that enter inside the method chosen (ε-NTU), for example the calculation of Global heat transfer coefficient *U*. In the following chapter, we analyzed the expressions available in the literature to calculate these parameters for the plate and fin heat exchangers.

## 3.7. Closure Relations

The main parameter to be defined, in order to apply both previous methodologies, is the global heat transfer coefficient, called *U*, defined as:

$$U = \sum R_h, R_{f,h}, R_k, R_c, R_{f,c} \tag{38}$$

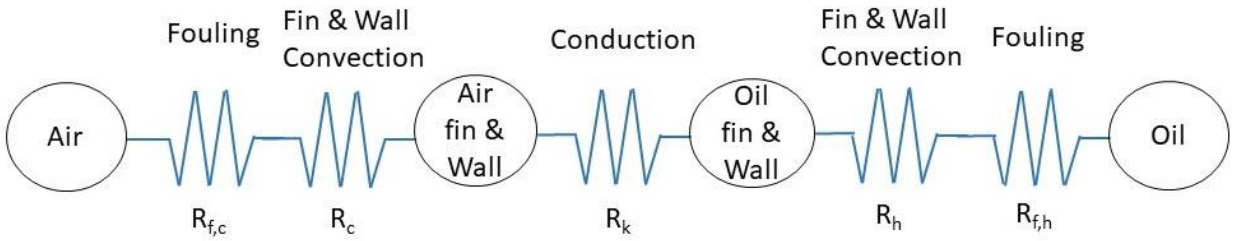


*Figure 24 - Schematic of the thermal exchange between two fluids (air and oil)*

where:

- $R_h$ is the thermal resistance that represents the convention between the hot fluid and the wall (this resistance is calculated with clear area). There is another resistance for the cold fluid ($R_c$).
- $R_f$ is the thermal resistance that represents the conduction between the fouling layer and the wall. It exists for both fluids.
- $R_k$ is the thermal resistance that represent the conduction across the metal thickness

Therefore, in the *U* parameter are included all mentioned effects, which in turn depend on other factors such as HTC. At this point, in following paragraphs it will be described what these thermal resistances represent and how it can be calculated.

### 3.7.1. $R_{h/c}$: convective resistance

The convective resistance for hot and cold fluid is calculated as follow:

$$R_{h/c} = \frac{1}{h_{h/c} * A_{h/c}}$$

where the parameter *h* is calculated with this formulation:

$$h_{h/c} = \frac{1}{HTC_{h/c} * LMTD_{corr} * \eta_{h/c} * A_{wet,h/c}} \tag{39}$$

where:

- HTC is the heat transfer coefficient and it is calculated using the dimensionless number: Nusselt (40). The Nusselt number is a function of Reynolds and Prandtl numbers of the fluid in interest (41).

$$Nu = \frac{HTC * L}{k} \tag{40}$$

$$Nu = j * Re * Pr^{1/3} \tag{41}$$

- $LMTD_{corr}$ is a correction factor applied to the logarithmic mean temperature value to consider non-linear channel geometry if present (e.g. several passages, see paragraph 3.2)
- $\eta_{h/c}$ is the overall fin efficiency and it is calculated as follows:

$$\eta_{h/c} = 1 - \frac{A_f}{A}\left(1 - \eta_f\right) \tag{42}$$

  where the $A_f$ is the entire fin surface area, $A$ is the overall thermal exchange area and $\eta_f$ is the efficiency of a single fin.
- $A_{wet,h/c}$ is the wetted area which is the area of the channel in contact with the fluid.

The calculation of convective resistance is complex and it is a function of different parameters, such as surface geometry, fluid properties and flow condition, which are difficult to be defined exactly for the case of interest. The same observation can be done for the Colburn factor ($j$, equation (41)), where the expression for its calculation has been studied in several papers available in the literature. Several papers define the expression of $j$ as a function of geometry parameters and dimensionless numbers (Reynolds and Prandtl number).

One of the possible expressions for the Colburn Factor calculation it is described in the study of Manglik et al. [5] that will be briefly explained in the following paragraph. The expression available in the paper, it will be used like an example for the explanation of how the model uses the equations inserted, which can not be displayed due to company intellectual propriety regulations.

### 3.7.2. Colburn factor (j) and Friction factor (f)

Many different correlations for heat transfer and pressure drop in offset strip fin heat exchangers have been reported in literature. Those correlations are based on a literature database that contain dissimilar geometries: scaled-up and actual offset strip fins, louvered fins, and finned flat tubes [5].

Manglik and Bergels analyzed the experimental data provided by Kays and London [6]. For each geometry, they defined the value of the geometrical parameters (α, δ, γ) to be included in the power law for calculating the Colburn factor (*j*) and the Friction factor (*f*) (Figure 25).

The Figure 26 shows the results of the parameters *f* and *j* for two pairs of surfaces, in which they share the same value of δ but have a different aspect ratio (α). It is observed that the influence of the parameter α is strong and this effect is equal both for laminar and turbulent flows. The value of the parameters *f* and *j* increase with the decrease of α. The thickness of the fin produces a disturbance in the flow (form drag) that affects the efficiency of the heat exchange and also it is observed that the boundary layer grows along the length of the fin and decays abruptly at the end of the length.

Therefore, for fins of reduced length and large thickness, it is observed that the flow moves outwards at the inlet and receives an acceleration at the outlet from the fin. Looking at the graph, Figure 27, the thickness and the length tend to have an opposite effect on the motion field. Thicker fins have larger form drag and provide an additional heat exchange in addition to what happens on the side walls [5], on the other hand, with longer and thinner fins, *f* and *j* are only affected by the amount of motion and heat exchange that occurs on the side walls. These phenomena are characterized by the parameter δ=t/l and are observed in Figure 28 where data are plotted for a pair of surfaces with the same α but different δ [5].

The fact of having thicker fins leads to smaller channels and, with the same width, to a lower fin density and a smaller passage area. The latter effect is attributed to the parameter γ=t/s [5].

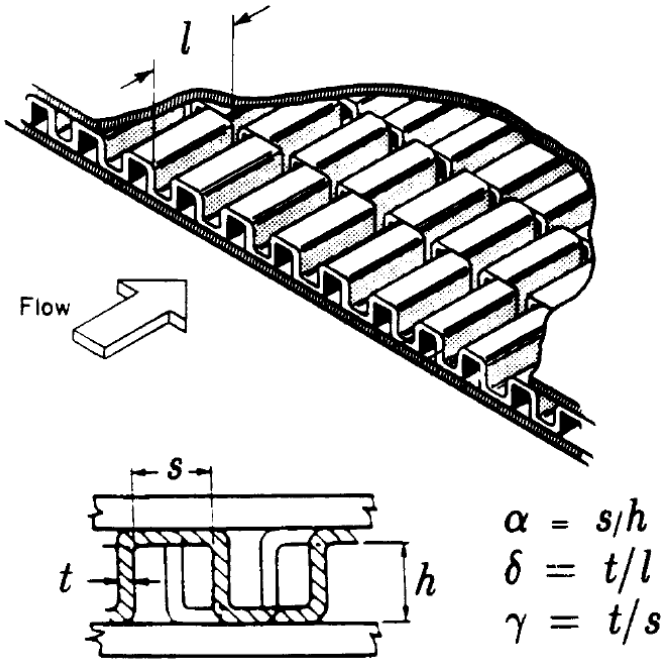


*Figure 25 - Geometrical description of a typical offset strip fin core [5]*

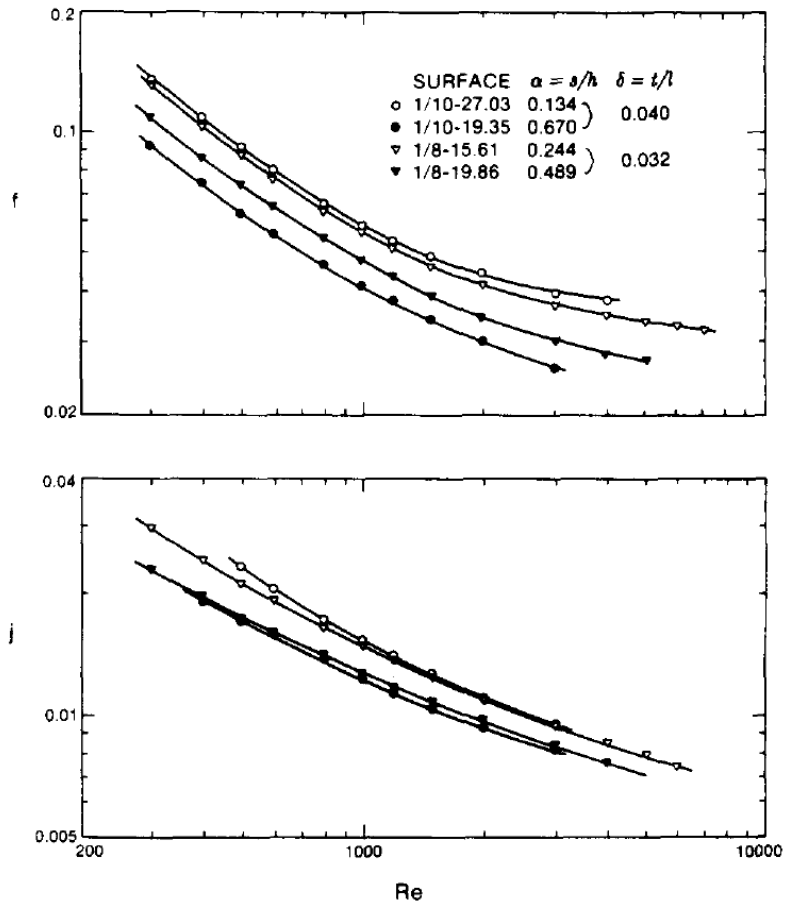


*Figure 26 - Effect of aspect ratio (α=s/h) in the experimental data for f and j [5]*

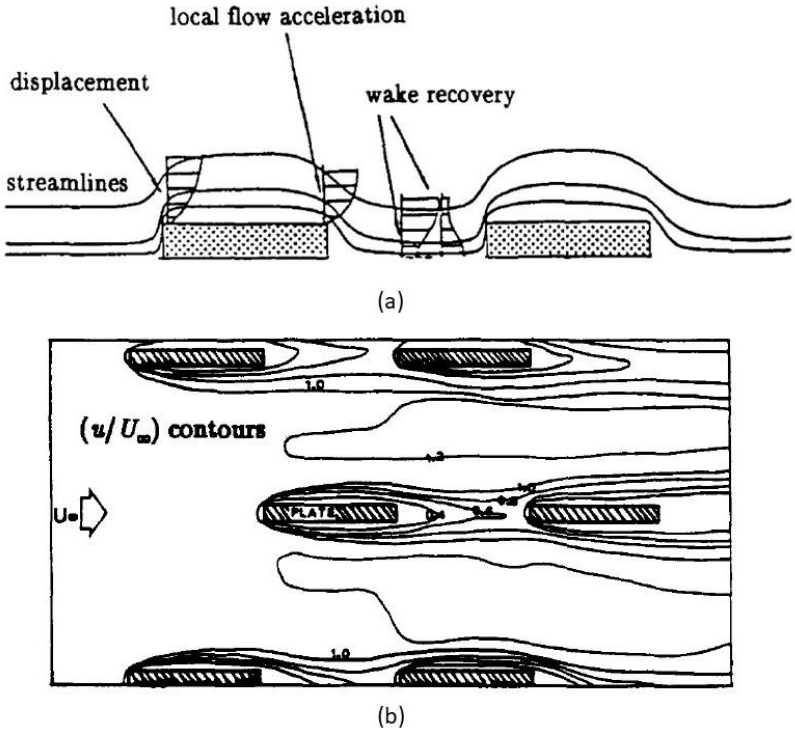


*Figure 27 - Schematic of the flow behavior in a typical offset fin array. (a) Growth and disruption of boundary layer; (b) isovelocity contours [5]*

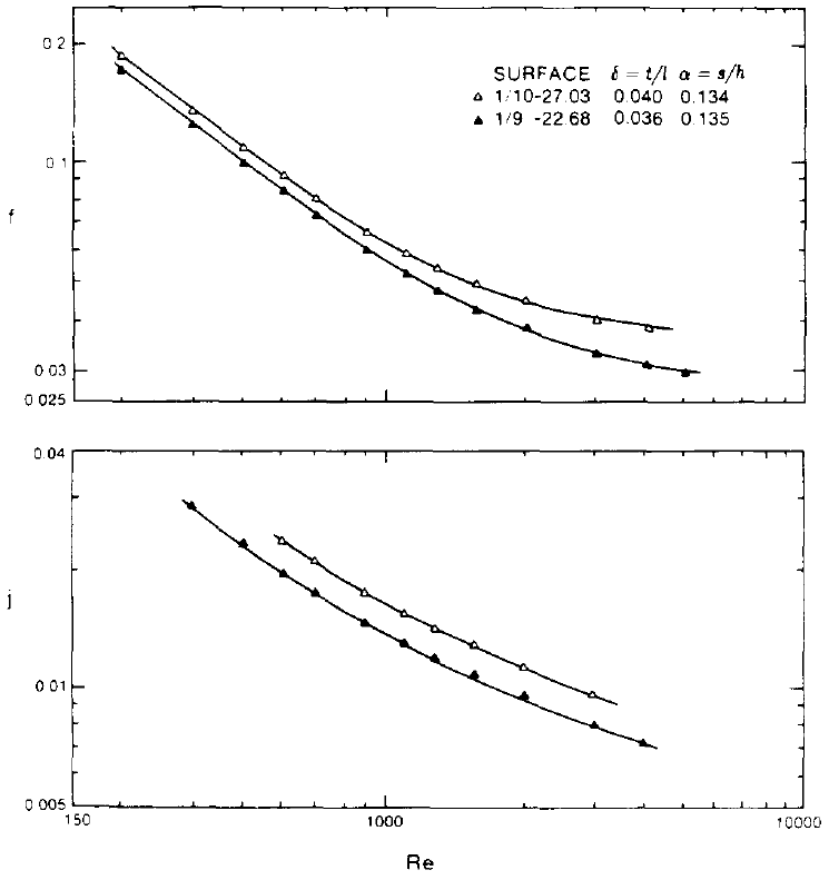


*Figure 28 - Effect of fin thickness/offset length ratio (δ=t/l) on the experimental data for f and j [5]*

From the previous explanation, it is evident that *f* and *j* are functionally related to Re, α, δ and γ and can be represented by these power law:

$$f = A * Re^{a1} * \alpha^{a2} * \delta^{a3} * \gamma^{a4} \quad [5]$$

$$j = B * Re^{b1} * \alpha^{b2} * \delta^{b3} * \gamma^{b4} \quad [5]$$

The previous charts show constant-slope log linear lines in laminar and fully turbulent flow conditions with no discontinuity, which is normally associated with the transition in the flow. Therefore, these expressions of the law of power can be used in both cases because the variations of parameters *f* and *j* as only a function of parameters Re, α, δ and γ.

Manglik and Bergels analyzed 18 geometries separately in the laminar and turbulent flow regions with air as working fluid to define the exponents and the coefficients to calculate *f* and *j* [5].

The law of power defined by Manglik is as follow [5]:

$$f = 9.6243 * Re^{-0.7422} * \alpha^{-0.1856} * \delta^{0.3053} * \gamma^{-0.2659} * [1 + 7.669 * 10^{-8} * Re^{4.429} * \alpha^{0.920} * \delta^{3.767} * \gamma^{0.236}]^{0.1} \quad [5]$$

$$j = 0.6522 * Re^{-0.5403} * \alpha^{-0.1541} * \delta^{0.1499} * \gamma^{-0.0678} * [1 + 5.269 * 10^{-5} * Re^{1.340} * \alpha^{0.504} * \delta^{0.456} * \gamma^{-1.055}]^{0.1} \quad [5]$$

These equations correlate the experimental data, identified by the authors, within $\pm 20\%$. These expressions describe the behavior of the offset strips up to the heat exchange and friction losses for all the flows, (i.e. laminar, transition and turbulent), and make it possible to avoid having to know the real flow for a specific working condition. These formulations could be adopted to evaluate the heat exchanger performances in off-design conditions.

The reported correlations are only exemplary equations that can be used to model the convective resistance of air/oil and the pressure losses inside the heat exchanger. Actual correlations inserted in the design tool for this thesis are voluntarily omitted due to company intellectual propriety regulations.

### 3.7.3. $R_f$: fouling resistance

For a heat exchanger the parameters of fouling and cleaning are very important especially in the case of heat exchanger where the fluids used are:

- liquid-liquid,
- if a phase change occurs during the exchange
- gas-liquid.

Fouling should be evaluated both in the design and off design points. The maintenance and replacement instructions of some heat exchangers sub-components are defined on the basis of the type of fluids used inside the heat exchanger and how easily the fluid form fouling.
Usually a plate heat exchanger has small hydraulic diameters and therefore as soon as a layer of fouling forms the performance is probably lower than design values. Clogging can also occur where one of the channels is blocked by the fouling and the fluid can no longer pass through the passage causing a deterioration of the heat exchange performance.
Thermal incrustation occurs in the presence of a temperature gradient, which produces a layer on the channel surface where the heat exchange is taking place.
The performance deterioration due to fouling effect is related to the formation of a fouling layer that adds a new thermal resistance (which may have been neglected during the initial design and usually it is a thermal insulation) that causes a decrease of the value of U. In addition to this, the pressure drops also increase, because the channel passage area is less compared to the initial design intent [6].

The fouling resistance for hot and cold fluid is calculated as follow:

$$R_f = \frac{f_{coeff,h/c}}{A_{h/c}} \tag{43}$$

where the parameter $f_{coeff,h/c}$ is a value found in literature and has been defined for the most common cases encountered during the design of heat exchanger.

As said before, the reported correlation is only exemplary equations that can be used to model the fouling resistance. Actual correlation inserted in the design tool for this thesis are voluntarily omitted due to company intellectual propriety regulations.

### 3.7.4. $R_k$: conductive resistance

In thermal conduction, the heat flow passes through the metal wall that separates the two fluids. In this resistance, the thermal conductivity of the material (which usually is metal) is involved. Usually materials with high heat conduction are used, therefore in most cases the value of this resistance is very slight compared to the resistances previously described.
The conductive resistance is calculated as follows:

$$R_k = \frac{1}{k_{metal} * \frac{A_{tot,vertical}}{t_{wall}}} \tag{44}$$

where:

- $k_{metal}$ is the metal thermal conductivity
- $A_{tot,vertical}$ is the heat exchange area
- $t_{wall}$ is the metal thickness

The reported correlation are only exemplary equations that can be used to model the conductive resistance. Actual correlation inserted in the design tool for this thesis are voluntarily omitted due to company intellectual propriety regulations.

In conclusion, the calculation of the parameter UA is:

$$U * A = \frac{1}{h_{air} + h_{oil} + k_{conduction} + f_{oil} + f_{air}} \tag{45}$$

## 3.8. Modelling of the pressure losses

One of the possible expressions in the literature for the calculation of pressure drops is available in the Kays and London [6], which is as follows:

$$\Delta p_{tot} = v_1 * \left[ (K_{in} + 1 - \sigma^2) + 2 * \left( \frac{v_2}{v_1} - 1 \right) + f \frac{A}{A_c} \frac{v_m}{v_1} - (1 - \sigma^2 - K_{out}) \frac{v_2}{v_1} \right] \qquad [6]$$

where:

- $K_{in}$ and $K_{out}$ are parameters that define the duct and they are available in the tables or charts
- $\sigma$ is the ratio between the free flow area to frontal area
- v is the velocity depending on the position (inlet, outlet, mean)

The reported correlation are only exemplary equations that can be used to model the total pressure drops. Actual correlation inserted in the design tool for this thesis are voluntarily omitted due to company intellectual propriety regulations.

In the following paragraph, it will be presented how the proposal model for the design of heat exchanger works. For the sake of clarity, during the explanation of the model, it will be used the reported previous equations as reference which are only an example to be more clear possible in the exposition of how the model works. Actual correlations inserted in the design model for this thesis are voluntarily omitted due to company intellectual propriety regulations.

# Chapter 4

# Design model adopted

The aim of this chapter is to provide an overview of 0D model developed in this thesis. In particular, the next sections will present the main assumptions, input and output parameters and the model approach used for the Heat exchanger design.
As internal company model, all the thermodynamic properties of the working fluids, the thermal correlations adopted for HTCs and pressure losses, are voluntarily omitted as confidential information.

## 4.1. Design model

The model proposed for the heat exchanger design is based on the ε-NTU method, available in literature. The model was built to be used for the design of heat exchanger with these characteristics:

- Fluids: Air and Oil
- Type: Plate and Fin – Counterflow – Both fluid unmixed

The activities performed to build up the model are the following:

- Implementation of thermal and fluid-dynamic correlations in a software environment such as Matlab/Octave
- Introduction of code adjustments to increase flexibility and allow the usage with different inputs:
    - Heat rejection (design application)
    - Oil temperature (data post-process)

The Figure 29 shows a schematic view of the main input and output parameters of this model. The air and oil inlet temperature (depending on the boundary conditions of the problem) and thermodynamic properties of both fluids are provided. Air has been considered as an ideal gas, the oil thermodynamic curves has been provided as function of the temperature, available internally or through thermodynamic tables. Additionally to these input, the model obtains several geometrical parameters including the overall geometry of the heat exchanger, the geometry of the channels for both fluids (channel dimensions, position, dimensions and density

of the fins). Furthermore, it is possible to provide the model the working condition parameters such as clogging and fouling.

By supplying all these inputs to the model, along with the oil volumetric flow and the air mass flow rates, the model provides as output several parameters including the thermal power exchanged, the oil and air outlet temperature and the pressure losses for both fluids.

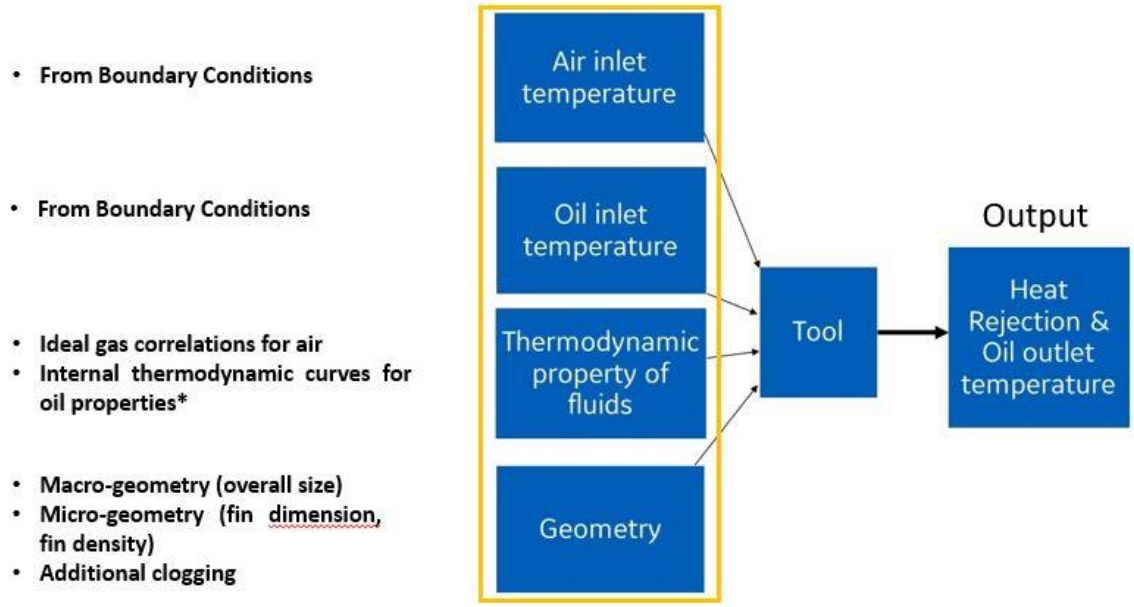


*Figure 29 – Outline of the inputs and outputs of the proposed model (*correlations adopted for thermal modelling, fluid dynamic modelling and fluids thermodynamic properties are voluntarily omitted due to company intellectual propriety regulations)*

## 4.2. Thermal model

In the model, thermal resistances due to conduction, convective and fouling have been taken into account, same procedure was followed for pressure losses. The details of the correlations implemented for the calculation of the thermal resistance, the pressure losses and the equations of the fluids thermodynamic properties have been voluntarily omitted due to company intellectual propriety regulations.

### Main assumptions

1. Air is modelled as an ideal gas. It is also assumed that air is taken directly from the atmosphere. Pressure and temperatures varies with the altitude.
2. Input of the model are the following:
    a. Heat power exchanged
    b. Oil volumetric flow
    c. Altitude

d. Air mass flow
e. Geometry of the heat exchanger

## 4.3. Modelling approach

The design model is based on the ε-NTU method (see paragraph 3.4). The procedure described below is generalized and the exact correlations used cannot be disclosed. Suppose to consider as input: oil and air flows, air inlet temperature and thermal power. The numerical procedure is the following:

1. Guess a desired value for the oil outlet temperature $T_{oil,outlet}$
2. All geometric parameters are calculated in order to have all the factors for subsequent calculations (hydraulic diameter, frontal area, etc.).
3. Evaluate the oil inlet temperature through the energy balance (equation (3)). Note that this is an iterative procedure, as equation (3) includes the average specific heat capacity $c_p$ of the fluid along the heat exchanger, that is a function of both inlet and outlet temperatures.
4. Apply the thermal correlations (not reported) for a preliminary estimation of the air and oil heat transfer coefficients $h$ for both fluids
5. Calculate fin efficiency for both air and oil (equation (42)) and the correction factor of LMTD (eq. (21) and the chart available in paragraph 3.2), to obtain the final values of $h$ for the fluids.
6. Calculate the thermal resistance caused by metal conductivity (equation (43))
7. Calculate the reduction in efficiency caused by the oil convection from the hot to the cold collectors along the heat exchanger (not reported)
8. Evaluate fouling contribution (equation (44))
9. Evaluate the final coefficient U multiply for the exchange area (equation (45))
10. Calculate the NTU (equation (26))
11. Calculate the effectiveness of the heat exchanger as a function of the NTU. The correlation used for the present tool is voluntarily omitted due to company intellectual propriety regulations. The literature equations can be found in paragraph 3.5 and in the Table 1. Example of using the effectiveness equation is in the paragraph 3.6.

12. Update the value of the oil inlet temperature, calculated as:

$$T_{oil,in} = T_{air,inlet} + \frac{W}{\varepsilon_{new} * C_{min}}$$

where the $C_{min}$ is the minimum thermal capacity among the two fluids, i.e.:

$$C_{min} = \frac{W}{\max[(T_{oil,in} - T_{oil,out}); (T_{air,out} - T_{air,in})]}.$$

13. With the new oil inlet temperature, the model calculates the new oil outlet temperature, because arrive at this point it is possible to calculate this temperature using the previous parameters:

$$T_{oil,outlet} = T_{oil,inlet} - \frac{W}{\dot{m}_{oil} * c_{p,oil,avg}}$$

The iteration ends when the oil outlet temperature coincides with the oil temperature desired defined in step 1 or the difference between exit oil temperature results in the two consecutive iterations are very low (the minimum error could be defined by the user).

# Chapter 5

# Validation with published experimental data

This chapter presents the validation of the proposal model with available literature data. In particular, the validation is carried out using the study of Hathaway et al [8].
The Figure 30 displays the geometry of heat exchanger. The main parameters used for the validation are the following:

- The overall length is 373 mm
- Total height is calculated through number of channels and channel height as in Figure 30, and it obtained 429.4 mm
- Same calculation for total width and it obtained 23.2 mm
- The oil microchannels are 38
- The oil fin thickness is 0.4 mm
- The oil fin length is 3 mm
- The oil fin number is 8 in width direction (from drawing)
- The air fin thickness is 0.1 mm
- The air channel width is 1.6 mm (from drawing the dimension is 1.7 mm and represent the fin thickness + passage channel and this information is finding also inside the document)
- The air fin height is 8 mm
- The oil channel width is 2.5 mm
- The oil channel height is 2.5 mm
- Gap oil fin is not declared and from drawing it only can be possible says that the value is smaller and near to zero. For this reason, it will be set to zero.

It has been assumed that additional surfaces (collectors/additional heat transfer surfaces) do not affect the heat exchange.

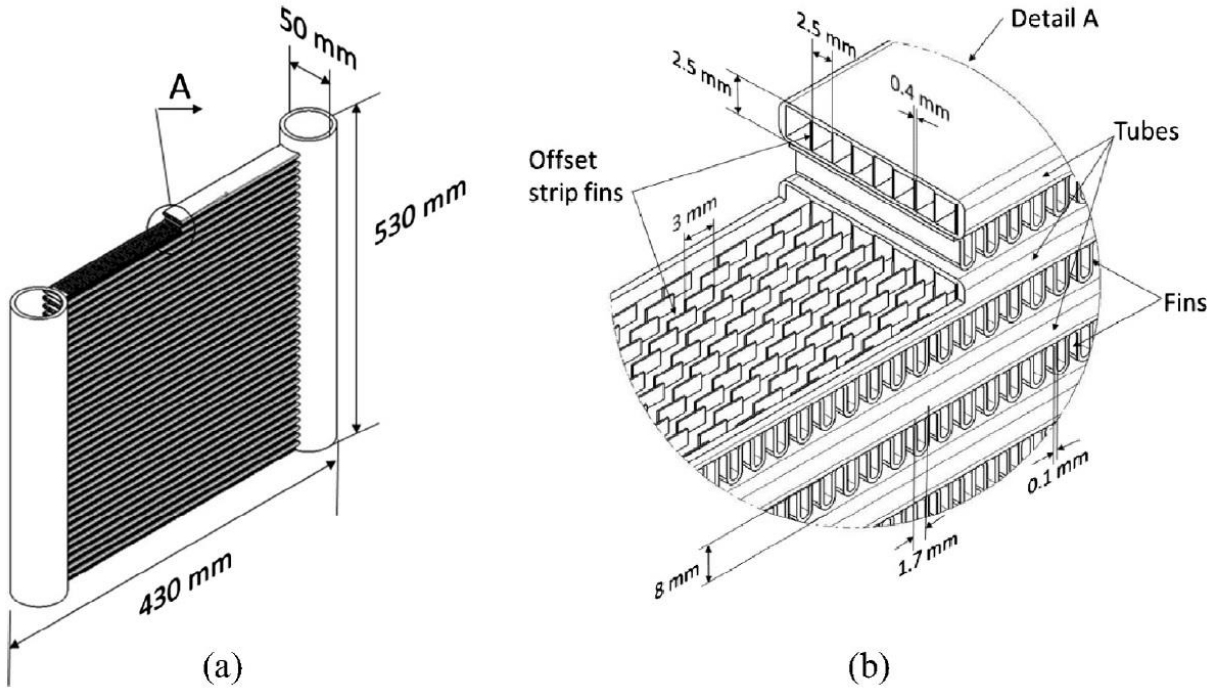


*Figure 30 - Stock microchannel aluminum oil cooler with plain fins on the air side and offset strip fins on the oil side: (a) overall dimensions, (b) microchannel detail [8]*

The paper data has been collected with the inlet air temperature equal to 318 K and the inlet oil temperature equal to 373 K. The stock heat exchanger is made by aluminum and the value of thermal conductivity is: 153.2 [W/m/K].

The "SAE 40 std" oil was used during the tests. To match the oil properties reported in the paper, especially the specific heat capacity, the oil chosen for the validation is the following: SAE 10W-40. The value of its properties, at temperature equal to 375 K, are:

- Density: the value is 810 [kg/m$^3$]
- Specific heat capacity: the value is 2184 [J/kg/K]
- Dynamic viscosity: the value is 0.010 [kg*s/m]

In Appendix A, has been reported the Table 4 with all oil properties in function of the temperature.

The comparison between the experimental data and the proposed model is carried out based on:

- Heat Duty and Global Heat Transfer Coefficient (UA) as a function of the air flow;
- $\Delta P_{air}$ as a function of the air flow;
- $\Delta P_{oil}$ as a function of the oil flow;

The paper data for these quantities are reported in the following figures: from 31 to 34. The comparison was made only with the curves called “Stock HX” (highlighted by the red circle). The other curves called “AM HX” were not considered.

- Heat duty

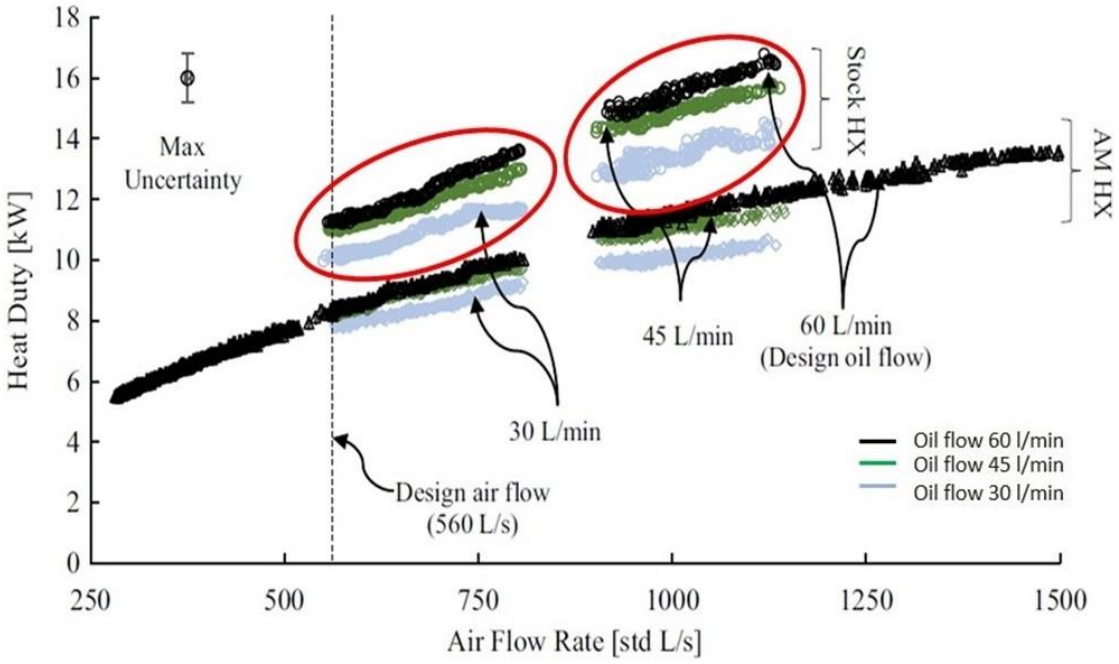


*Figure 31 – Heat duty as function of air flow [8]*

- Global transfer coefficient (UA)

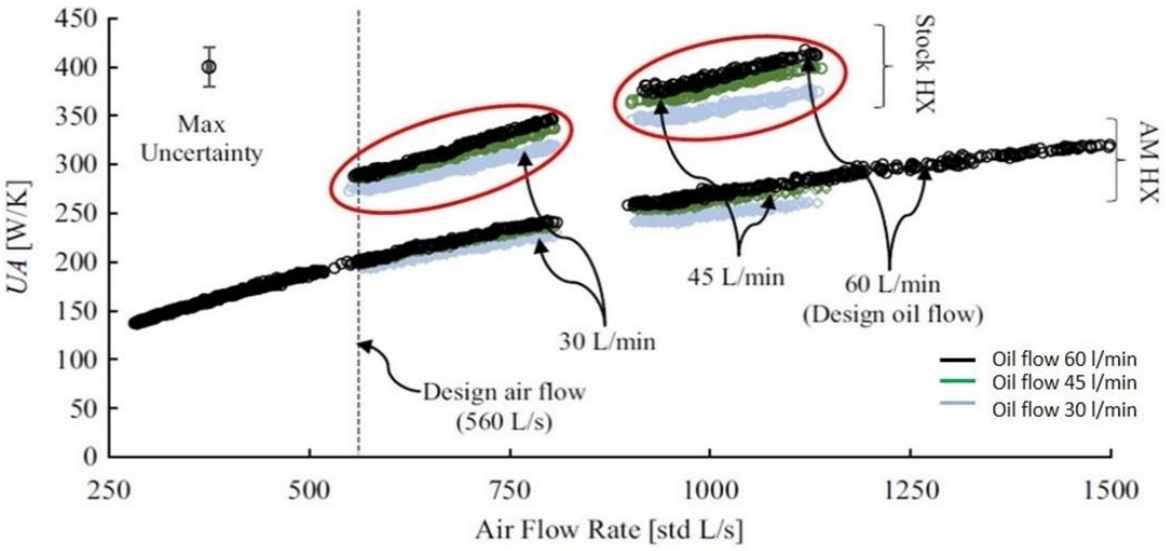


*Figure 32 – “Global heat transfer coefficient multiply area” as function of air flow rate [8]*

- $\Delta P_{air}$ as a function of the air flow

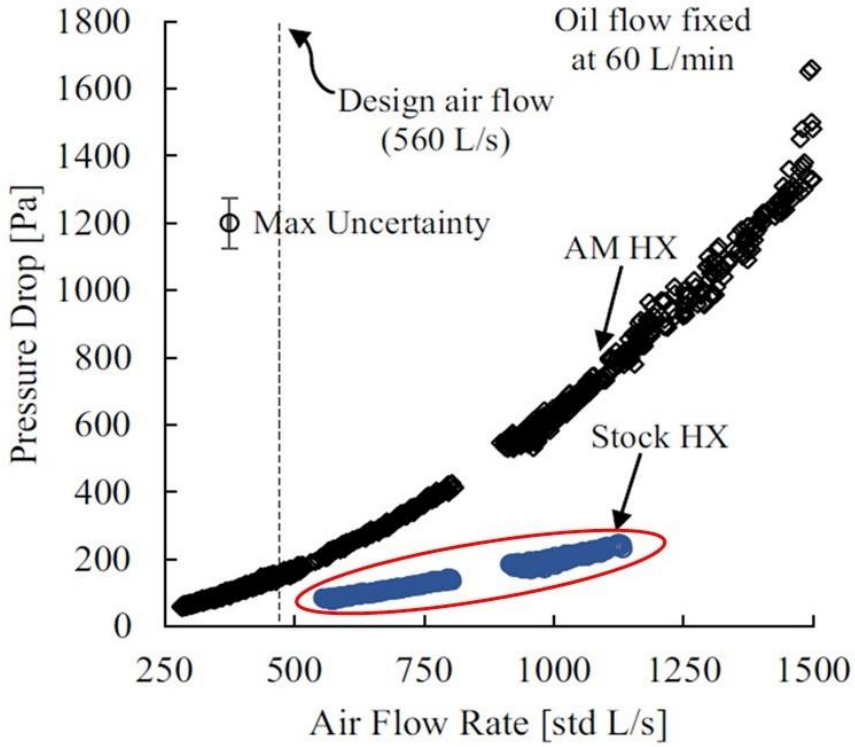


*Figure 33 – Pressure drop across the air side with oil flow equal to 60 l/min [8]*

- $\Delta P_{oil}$ as a function of the oil flow

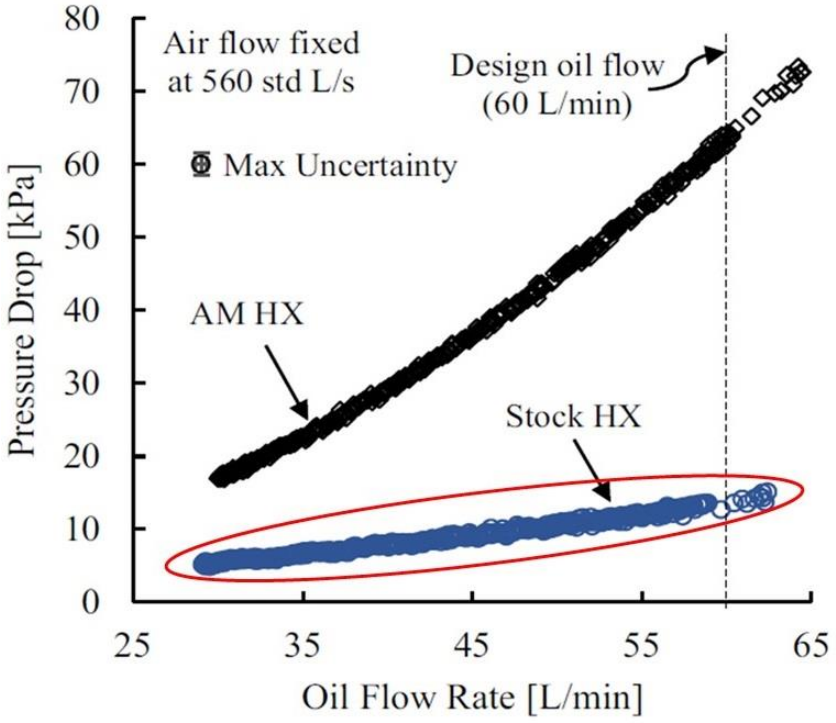


*Figure 34 – Pressure drop across the oil side with air flow equal to 560 std l/s [8]*

# 5.1. Case Study

## 5.1.1. Heat Duty predicted vs Paper data

This section describes the comparison for the quantity Heat Duty between the value predicted by the model and the paper data for all oil flow conditions (60-45-30 [l/min]). The comparison is carried out extracting the points from the charts in the paper. The expression for the calculation of the Heat Duty parameter is not displayed due to company intellectual propriety regulations.

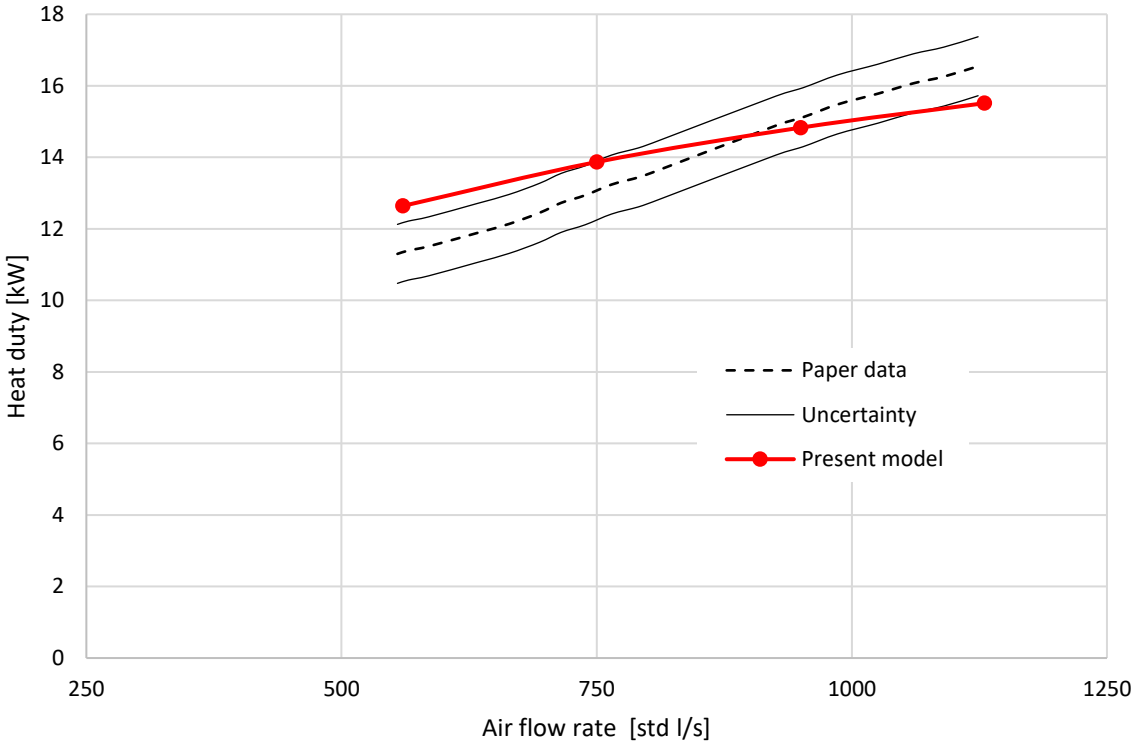


*Figure 35 – Heat duty with oil flow 60 l/min (constant) as function of air flow*

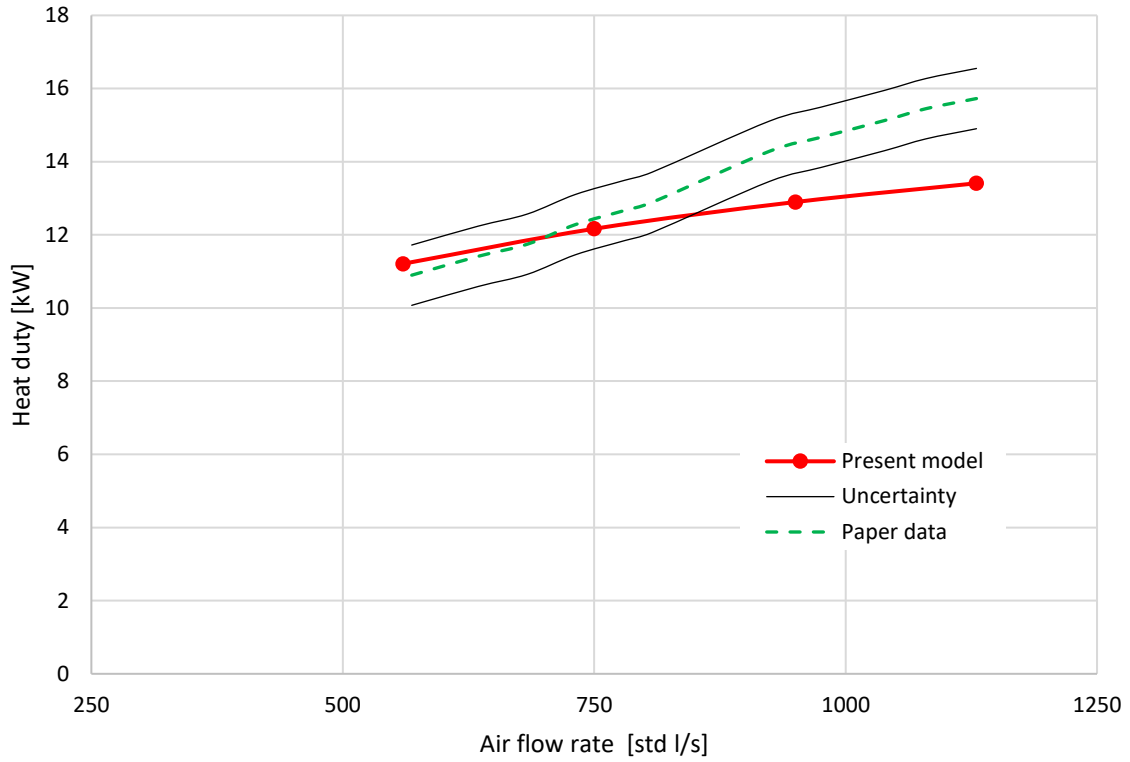


*Figure 36 – Heat duty with oil flow 45 l/min (constant) as function of air flow*

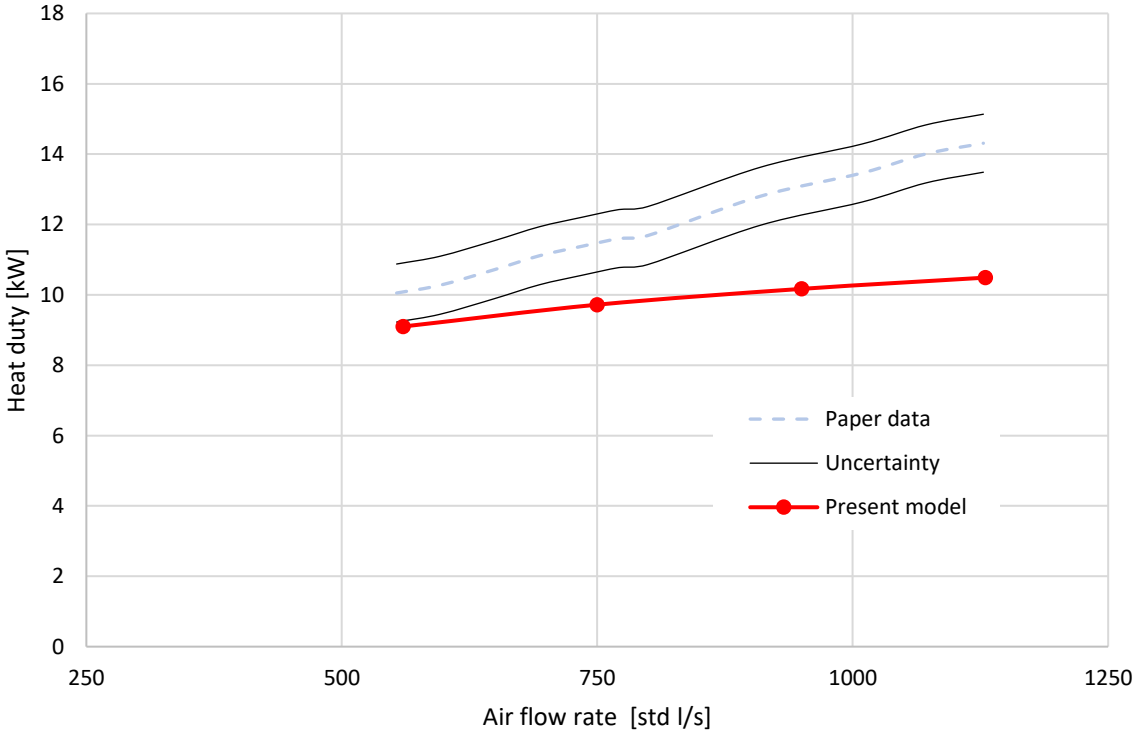


*Figure 37 – Heat duty with oil flow 30 l/min (constant) as function of air flow*

For the oil flow equal to 60 l/min, the value of the heat duty provided by the model at the design point is equal to 12.40 kW [Figure 35] whereas in the paper data the value is 11.5 kW. Therefore, between the prediction and paper data, the difference is 8%.

The results for the 45 l/min and 30 l/min oil flow cases will be discussed in the following paragraph.

### 5.1.2. Notes on data for cases: oil flow 45 l/min and 30 l/min

The Figure 36 shows, in the design point, that the model provide result comparable with what provided in the paper. Instead, for the case with oil flow equal to 30 l/min, the Figure 37 shows an underestimation for all points. In particular, in the design point, the model predicts a Heat Duty equal to 9.10 kW whereas the value from paper data is equal to 10 kW, therefore the error is -9%.

It should be noted that the latter case (30 l/min) has a low oil flow in relation to a high air flow. Analyzing the results achieved, I focused mainly on the discrepancy observed on the heat duty in the case of oil flow rate equal to 60 l/min. The others oil flows (45-30 l/min), due to the very high viscosity of the oil have low velocity. Reynold number for these low velocity cases is very low and it does not fit into the validity range of correlation selected (which is not reported due to company intellectual propriety regulations). The oil velocity value and Reynolds numbers for these two oil flows, are shown in the Table 2. For the design point (60 l/min), the Reynolds number is near the range of correlation; therefore, underestimation is less severe compared to the others oil flows.

| Oil flow rate [l/min] | Reynolds number | Velocity [m/s] |
|---|---|---|
| 60 | 93 | 0.54 |
| 45 | 68 | 0.40 |
| 30 | 45 | 0.27 |

*Table 2 – Reynolds numbers and velocity for all oil flow rate*

The underestimation of Heat Duty observed for these two low flow rates is arguably due to the fact of being outside the validity range of the correlation used. With low values of Reynolds, the dominant phenomenon in the heat exchange is no longer convection but conduction due to slow oil motion.

In addition to this phenomenon, the internal geometry of the channels is outside the validity range of correlation used (not reported due to company intellectual propriety regulations). This may be another factor to take into account as far as the different trend is concerned, but it will certainly have less impact than the Reynolds number.

For these listed reasons above, in the following paragraphs will only analyze the results obtained with the oil flow rate equal to 60 l/min.

### 5.1.3. Global transfer coefficient (UA) predicted vs Paper data

This section describes the comparison between the predicted results and the paper data for the UA parameter with oil flow equal to 60 l/min as function of air flow. The expression for the calculation of the UA parameter is not displayed due to company intellectual propriety regulations.

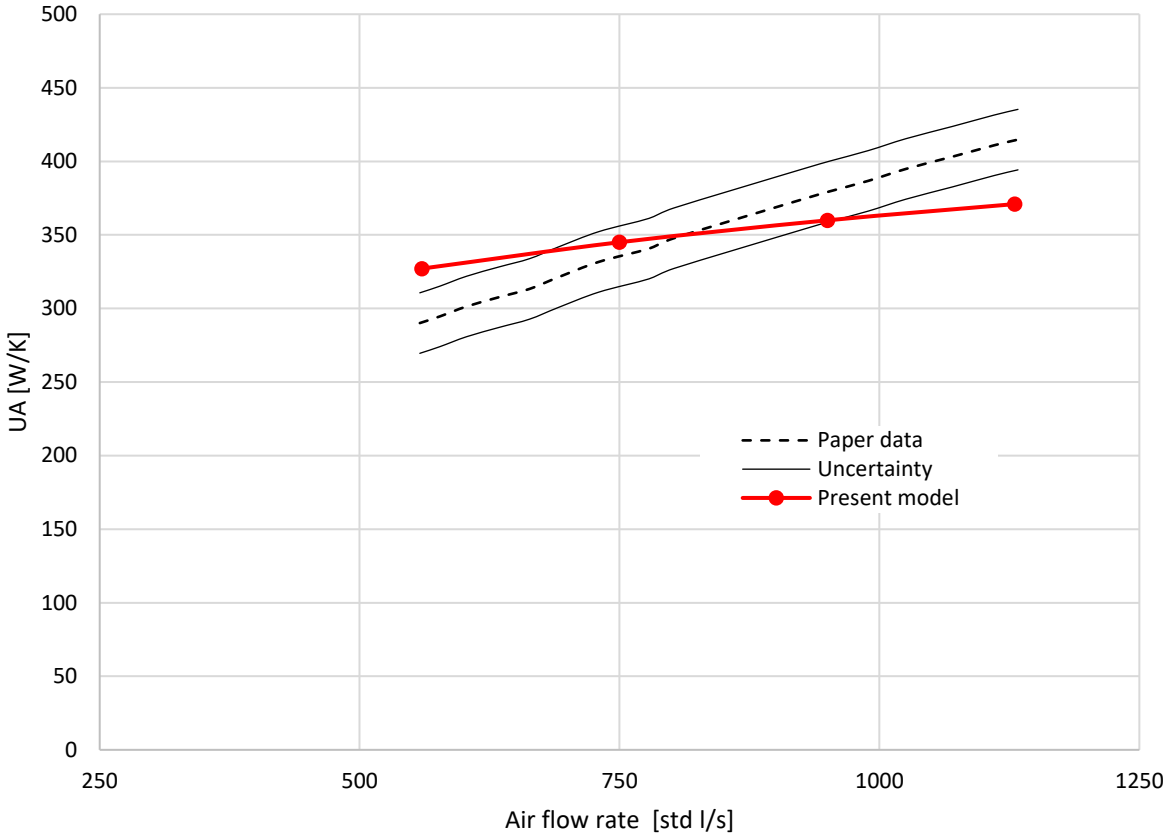


*Figure 38 – UA with oil flow 60 l/min (constant) as function of air flow*

Figure 38 shows that at the design point the value of UA predicted is 327 W/K and from the paper data is 293 W/K, so the difference is 12%.

It should be noted that the difference between paper data and model data increase as the air flow raises, the same thing that is seen in the Heat Duty analysis.

### 5.1.4. $\Delta P_{air}$ predicted vs Paper data

This section describes the comparison between the predicted results and paper data for the $\Delta P_{air}$ as a function of the air flow. The calculation of the $\Delta P_{air}$ is done using a formulation that cannot be displayed due to company intellectual propriety regulations. The paper data reported in the comparison chart is carried out using the interpolation from the $\Delta P_{air}$ paper chart available in the document.

In the design point, the air pressure drop from paper data is 75.4 Pa with an oil flow rate of 60 l/min. If the air flow rate rises to 1130 std l/s, the pressure drop is 235 Pa. The model provides at the design point a value of 60 Pa, and at maximum air flow rate a pressure loss of 222 Pa.

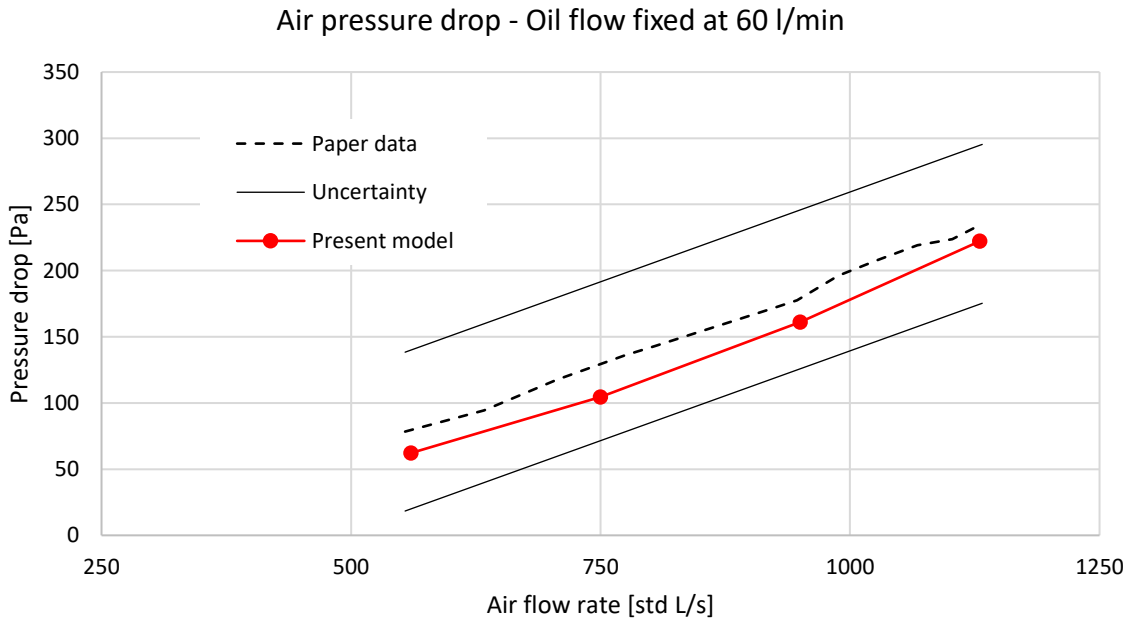


*Figure 39 – Pressure drop across the air side with oil flow equal to 60 l/min (constant)*

The trend of pressure drop coincides with what reported in the paper, therefore the model results are in good agreement with the paper values in terms of air pressure drop. The discrepancy is less than 30 Pa on all points.

### 5.1.5. $\Delta P_{oil}$ predicted vs Paper data

This section describes the comparison between the predicted results and paper data for the $\Delta P_{oil}$ as a function of the oil flow. The calculation of the $\Delta P_{oil}$ is done using the expression that cannot be displayed due to company intellectual propriety regulations.

In the design point, the oil pressure drop from the paper data is equal to 0.15 bar with an air flow equal to 560 std l/s. If the oil flow has decreased to 30 l/s, then the oil pressure drop is equal to 0.05 bar. The model predicted a value in the design point equal to 0.19 bar and a value for the lowest oil flow equal to 0.08 bar.

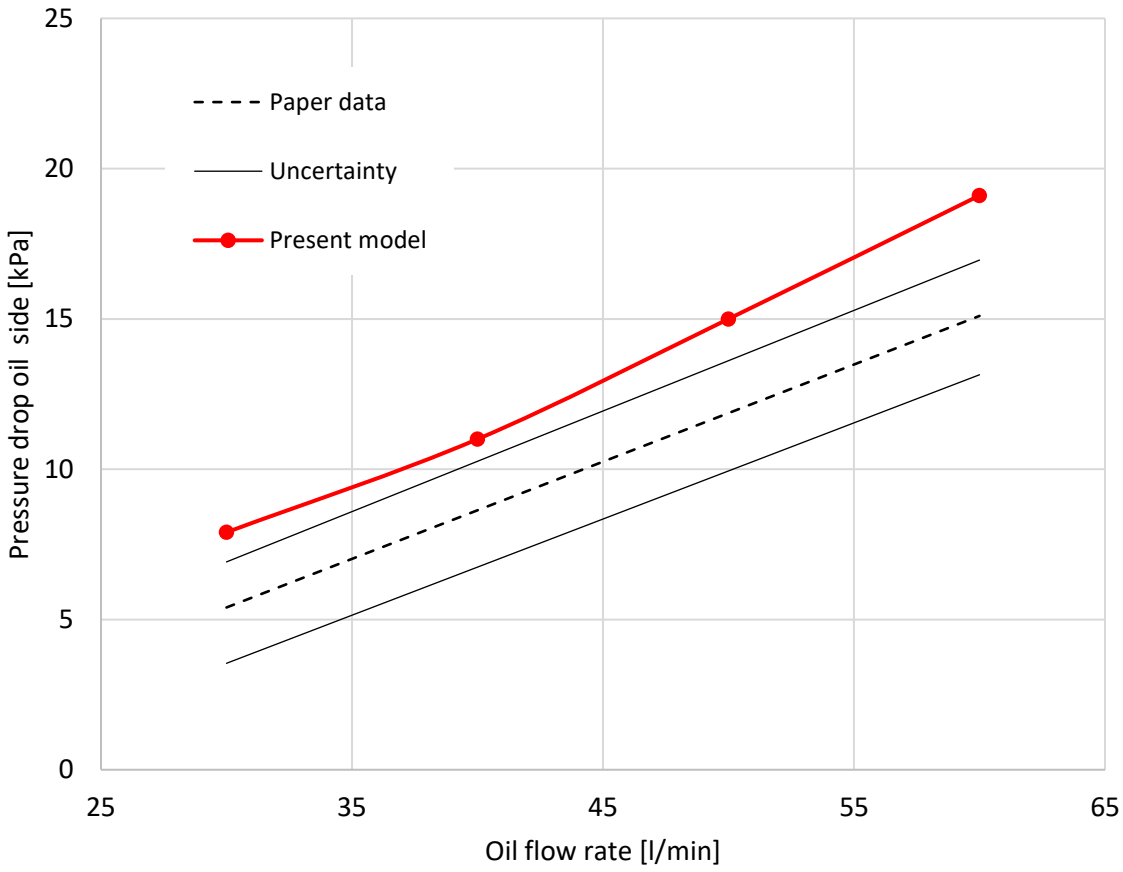


*Figure 40 - Pressure drop across the oil side with air flow equal to 560 std l/s (constant)*

The trend of pressure drop coincides with what reported in the paper, therefore the model results are in good agreement with the paper values in terms of oil pressure drop. The discrepancy is less than 0.05 bar on all points.

## 5.2. Discussion

The model results has been compared with the data found in literature. The comparison has been discussed in the previous paragraphs and a summary of the main outcomes are reported:

- Good agreement in terms of air pressure drops (<30 Pa on all points)
- Good agreement in terms of oil pressure drops (<0.05 bar on all points)
- The error on Heat duty is +8% in design point and -6% at high air flow rate for the oil flow equal to 60 l/min

The model uncertainties are linked to the inputs obtained from the paper and the method used. Assuming that the inputs provided are exact (geometry and fluid thermodynamic properties), the final error is mainly due to the uncertainties of the correlations used.

The correlation used for the oil HTC calculation (is not reported due to company intellectual propriety regulations), have an uncertainty of ± 20%. The air HTC correlation has an uncertainty of ± 10% (the expression is not displayed due to company intellectual propriety regulations). The Heat Duty graphs with these uncertainties applied are reported in the following pages. The uncertainties have been considered individually because the uncertainty of the single correlation is already very wide and takes into account many factors that may not have been properly evaluated during the analysis.

➢ *Uncertainty on oil HTC*

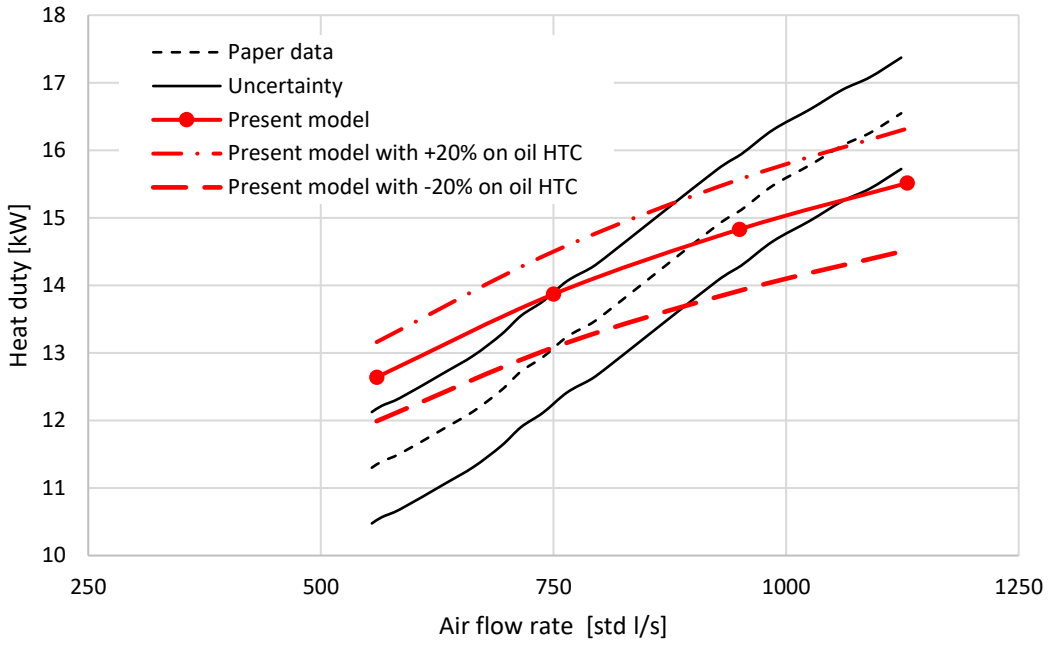


*Figure 41 – Analysis of Oil HTC uncertainty*

➢ *Uncertainty on air HTC*

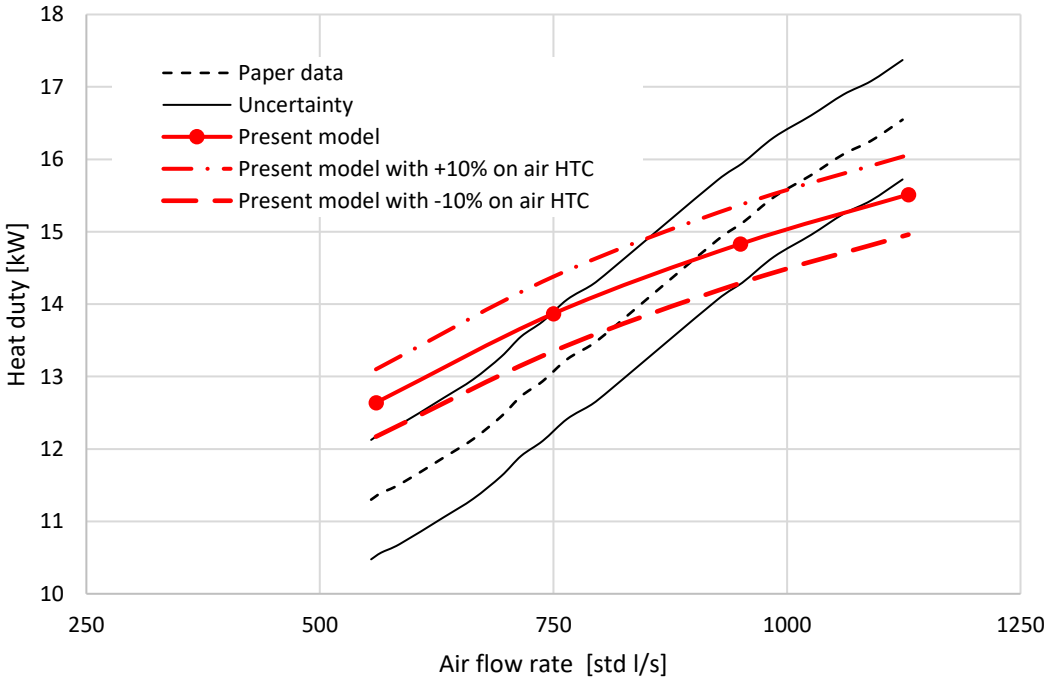


*Figure 42 – Analysis of Air HTC uncertainty*

Even applying the uncertainties on the results obtained from the model, there is always a different trend among the paper and model data. The difference, in absolute value, on the reference points is less than 10%.

The different behavior can be caused by:

a) misinterpretation of input data (geometry, thermodynamic properties of oil, etc.)
b) error in correlations or method used in the model

A deeply investigation has been conducted to understand which parameter causes the different trend and what this error is attributable to and for this aim a sensitivity analysis has been performed.
Firstly, the sensitivity analysis was used to check that the model provide results corresponding to the variation of the inputs provided (physical model implementation). In a second phase, the results from the analysis has been used to verify if the input parameters has an influence on the different behavior observed between paper and predicted data.
The sensitivity analysis selected are as follows:

1. Geometry
2. Oil property
3. Heat transfer coefficient

Each sensitivity analysis effect on the model results will be described in the following paragraphs. The air pressure losses are not included in the analysis because as shown in the previous sections of the thesis the model predictions are in line with the literature data.

## 5.3. Sensitivity Analysis

The sensitivity analysis was performed with two main objectives:

1. Verify the performance quality of the model
2. Analyze the impact of main factors on the final thermal power trend

In the following paragraphs, I will refer to the model without modification with the name: ***Reference model***.
All analysis has been performed only with an oil flow equal to 60 l/min due to the reasons described in the section 5.1.2.

### 5.3.1. Geometry

Two geometries were considered with regard to the oil channels. These two geometries have the following dimensions:

- **Case 1:** oil channel width is 2.1 mm and the oil channel height is 2.1 mm
- **Case 2:** oil channel width is 1.7 mm and the oil channel height is 1.7 mm

These values were selected based on the initial width and height of the reference geometry (2.5 mm) and the oil fin thickness equal to 0.4 mm.
The overall height and width of each heat exchanger are calculated using the values reported before.

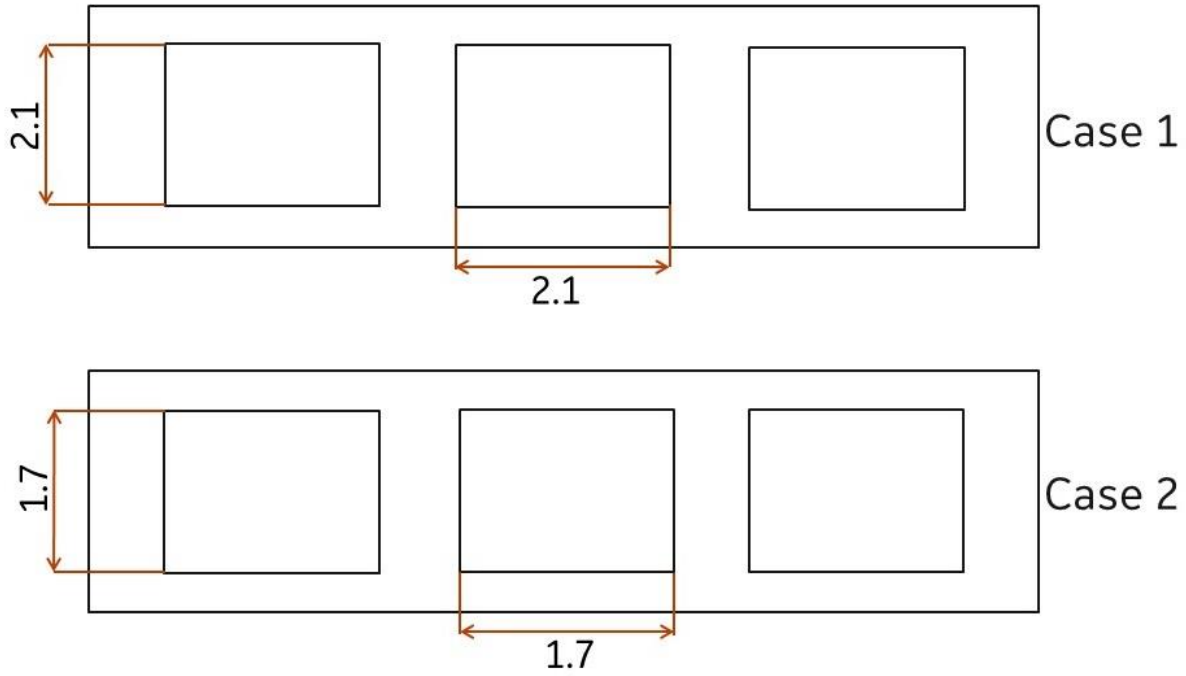


*Figure 43 - Dimension of oil channel for the two cases*

- ***Case 1:*** *Oil channel width and height are 2.1 mm*

The model predictions are reported in terms of Heat Duty in Figure 44 and for oil pressure drop in Figure 45:

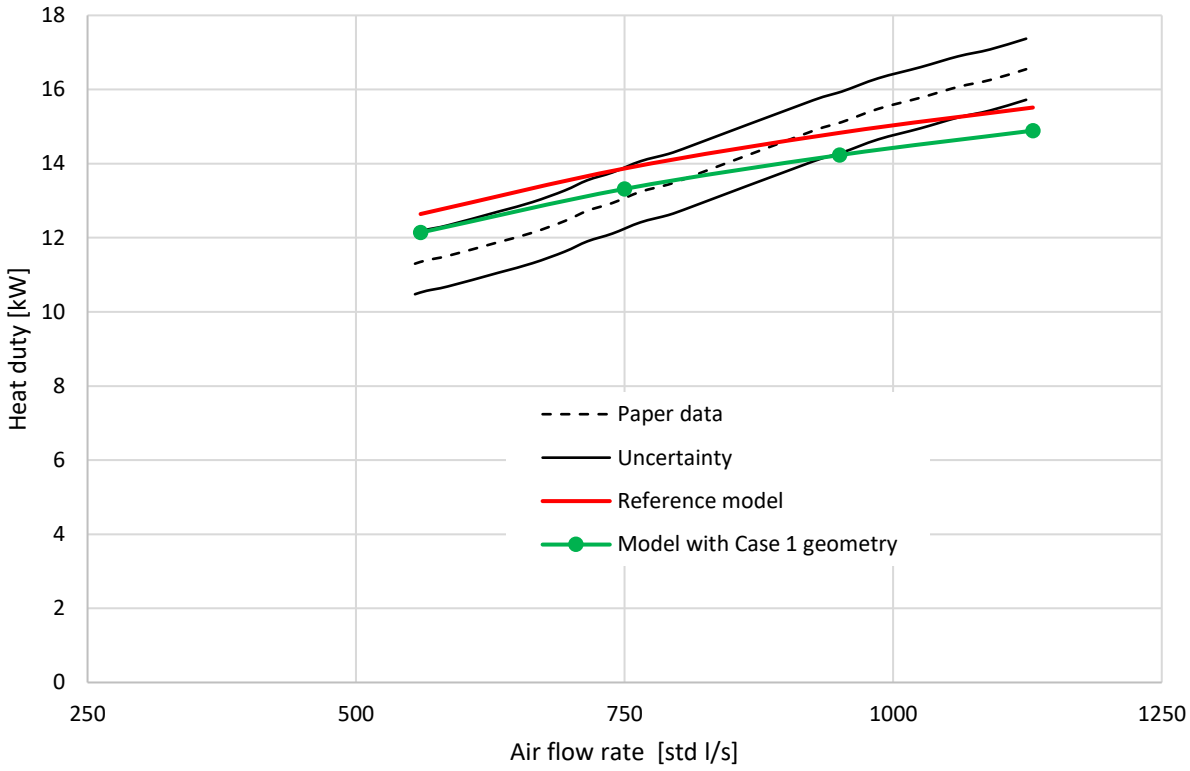


*Figure 44 - Heat duty with oil flow 60 l/min (constant) as function of air flow – Case 1*

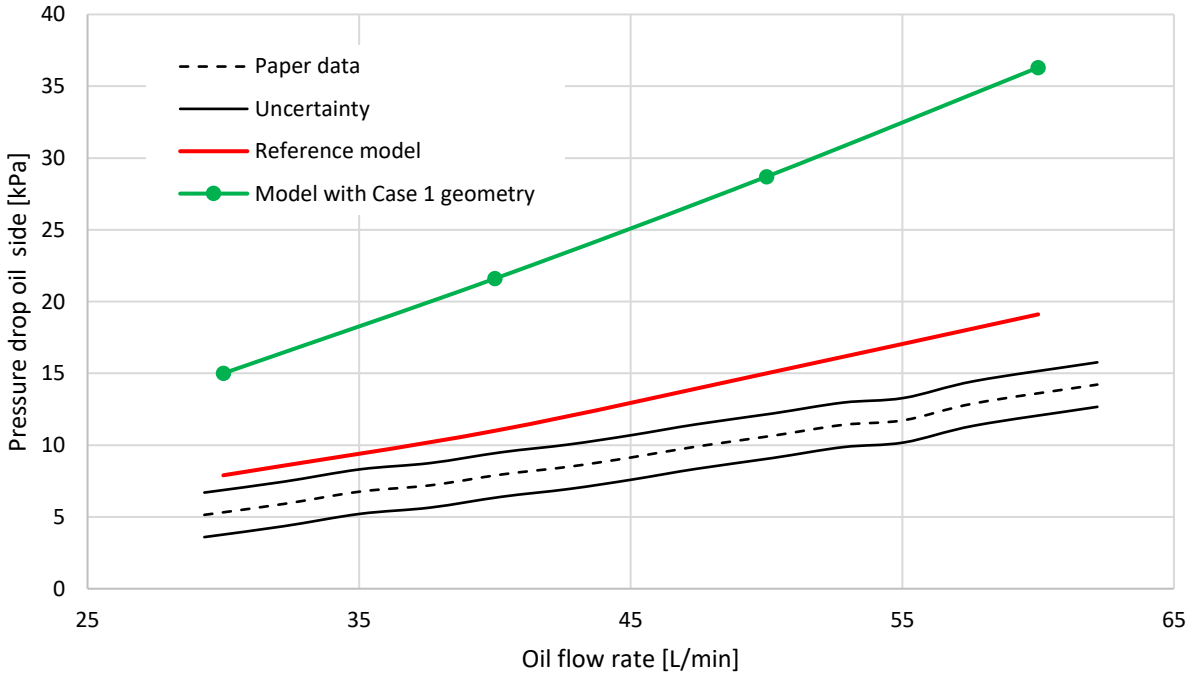


*Figure 45 – Oil pressure drop with air flow fixed at 560 std l/s – Case 1*

The oil channel is smaller with respect to the reference geometry, therefore the oil velocity will be higher with an increase in pressure losses. The velocity increment leads to a slight increase in the value of oil HTC (due to the Reynolds number variation), but this gain has a lower impact

than the reduction in the exchange area. For this reason, a slight decrease in Heat Duty can be observed.

- ***Case 2:*** *Oil channel width and height is 1.7 mm*

The Figure 46 and 47 shows the results obtained from the model for Heat duty and oil pressure drop respectively:

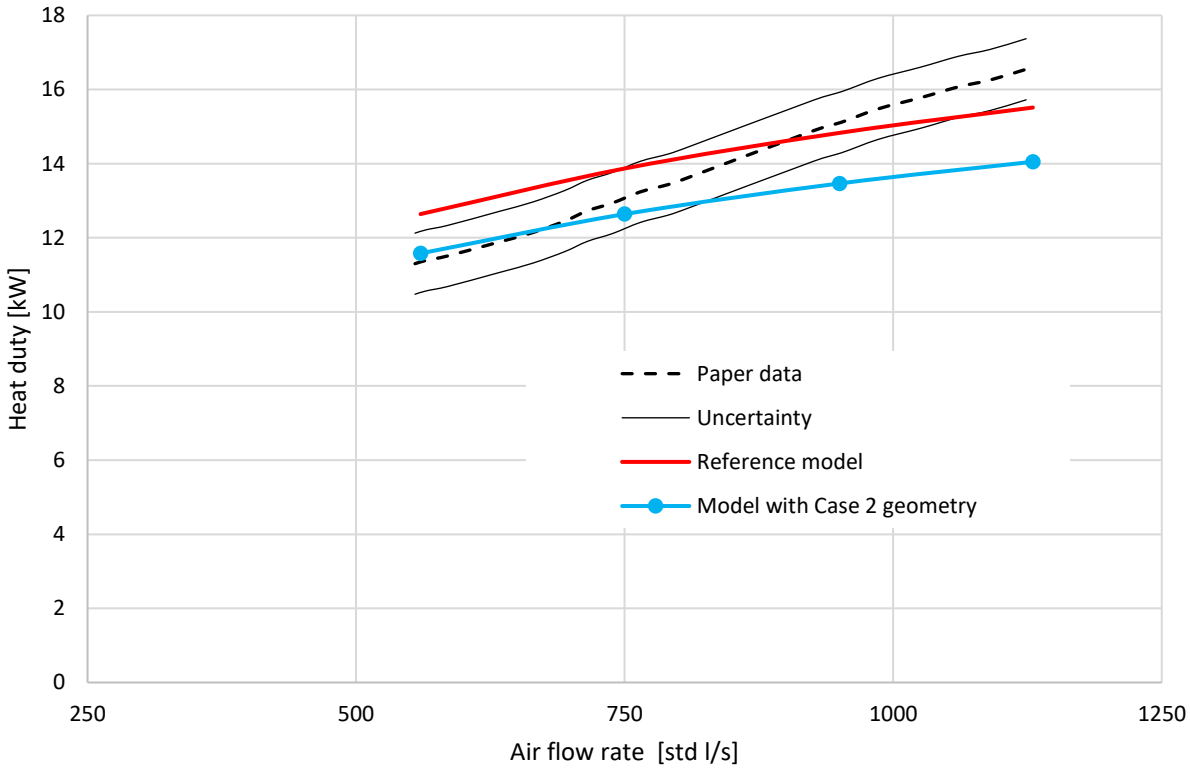


*Figure 46 - Heat duty with oil flow 60 l/min (constant) as function of air flow – Case 2*

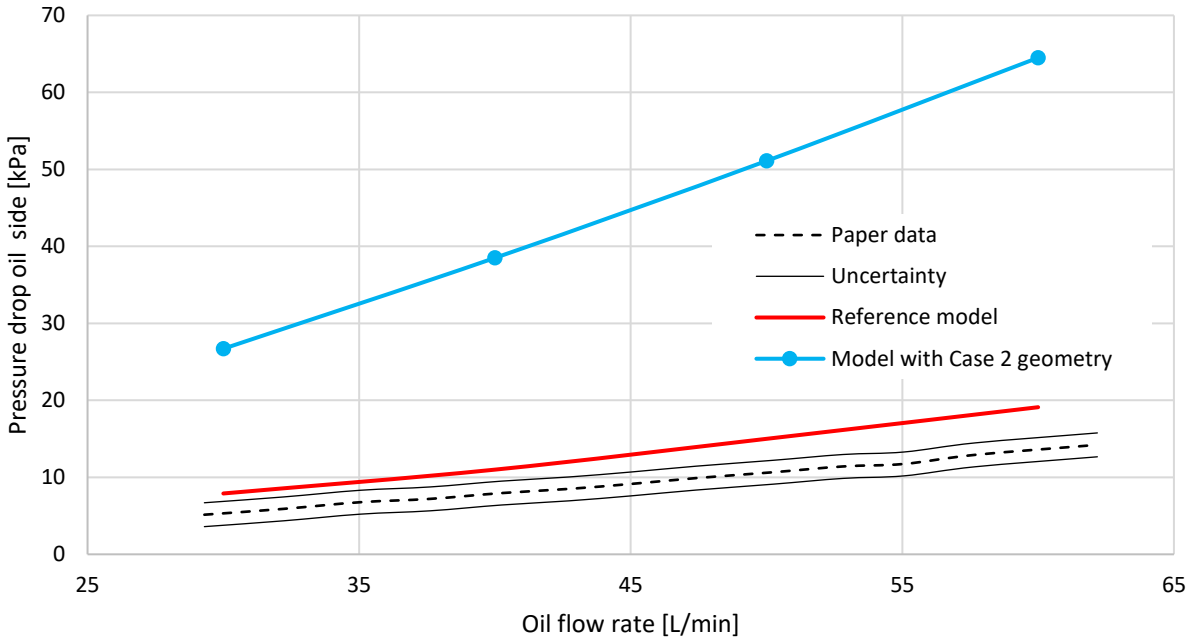


*Figure 47 - Oil pressure drop with air flow fixed at 560 std l/s – Case 2*

The Case 2 has a further reduction in oil channel size and therefore a reduction of the exchange and the passage area with respect to the Case 1. The Heat Duty calculated is lower than Case 1, but the oil pressure drop is higher due to the smaller channel passages.

The sensitivity analysis on the geometry parameters confirms that the model provides correct results and variation linked to the different input provided. The plots shows that a geometry variation of the heat exchanger dimension has not a big impact on the final performances, despite of that it is possible to notice that the performances of the two smaller heat exchanger are worst respect to the reference one.

### 5.3.2. Oil property

The second sensitivity analysis has been done acting on the oil properties. The paper [8] does not provide a complete description of the working oil used for the tests, therefore, an additional analysis was carried out using a second oil, namely "SAE 15W-40", to highlight the impact of the oil properties on final performance. The second oil considered belongs to the same family as the one initially considered (SAE 10W-40).

As mentioned above, this sensitivity analysis was done to observe whether the proposed model works consistently with the input provided.

The Table 3 shows the comparison of the properties at the reference temperature between the oil chosen and the other oils investigated (the Table 5 with all values for the new oil selected is reported in the Appendix A):

| | Density (T=375 K) $[kg/m^3]$ | Specific Heat Capacity (T=375 K) $[J/(kg*K)]$ | Dynamic viscosity (T=375 K) $[kg*s/m]$ |
|---|---|---|---|
| Paper oil | 851 | 2190 | 0.016 |
| Present Model (SAE 10W-40) | 810 | 2184 | 0.010 |
| SAE 15W-40 | 844 | 2138.8 | 0.012 |

*Table 3 – Properties of selected different oils*

The Heat Duty is reported in the Figure 48 and the oil pressure drop is reported in the Figure 49:

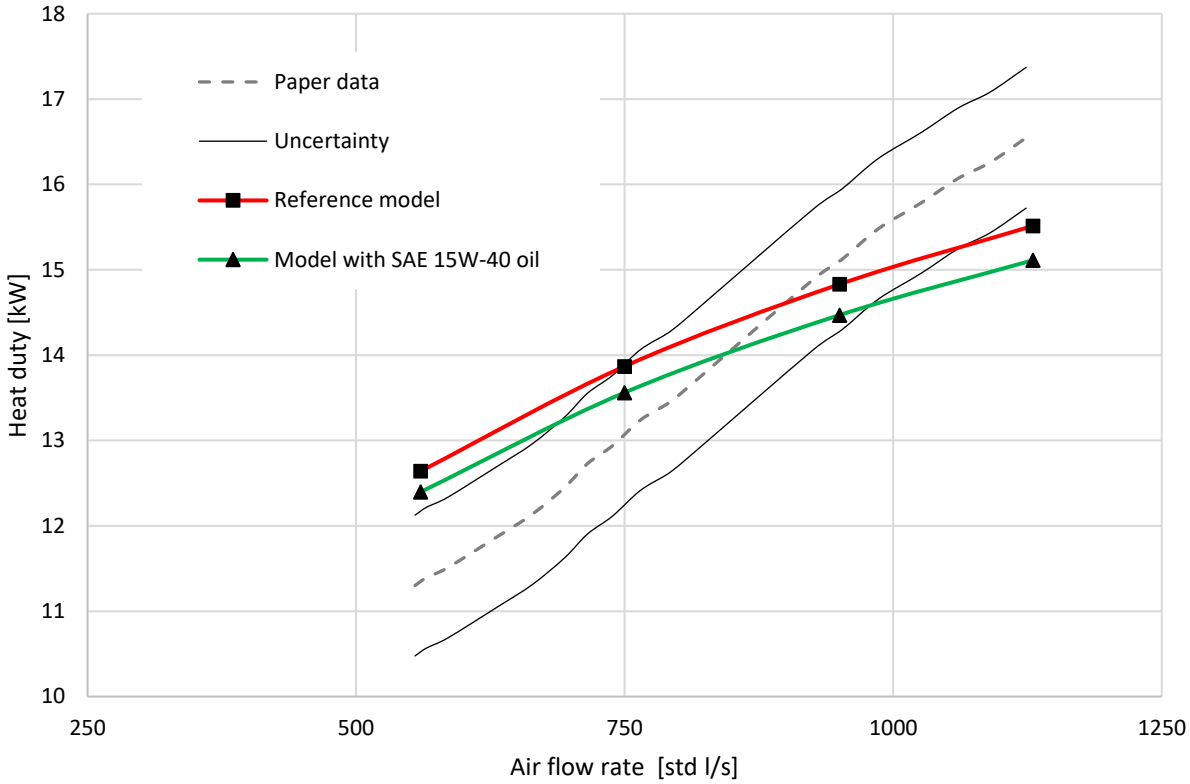


*Figure 48 – Heat duty with oil flow fixed at 60 l/min – Geometry: Reference case*

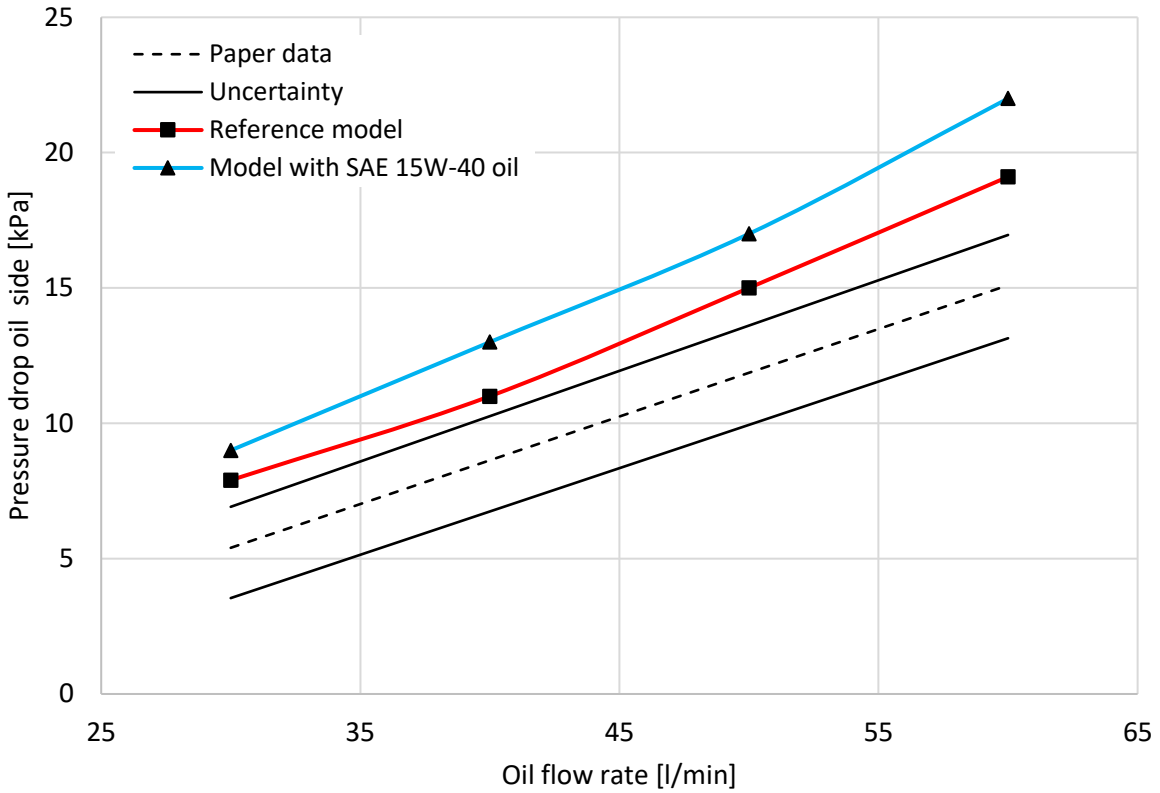


*Figure 49 - Oil pressure drop with air flow fixed at 560 std l/s – Geometry: Reference case*

The SAE 15W-40 oil has a higher viscosity compared to the reference case causing an increase in pressure drop. The value of the Heat Duty does not vary significantly even if the oil has a lower velocity. These results could be justified observing the SAE 15W-40 oil thermodynamic properties that influence the dimensionless numbers and therefore the heat exchange.

The behavior observed in the reference case is replicated also with different type of oil. The case analyzed provides worst results respect to the reference case, especially for the pressure drop. The sensitivity analysis on the oil properties confirms that the model provides correct results and trend with an input variation but it has not enough impact to justify the different behavior seen on the Heat Duty.

### 5.3.3. Additional notes: Impact of the oil viscosity

For the sake of completeness, a sensitivity analysis was done only on the oil viscosity, which is one of thermodynamic property with the highest uncertainty in terms of modelling. Oil viscosity enters directly in both Reynolds and Prandtl numbers for the fluid, therefore has a high impact on the HTC and on the pressure losses. The Figure 50 shows a comparison between four different calculations, carried out with:

i) nominal viscosity of SAE 10W-40 reported in Appendix A

ii) viscosity of SAE 10W-40 reduced by 10%

iii) viscosity of SAE 10W-40 increased by 10%

iv) viscosity of SAE 10W-40 increased by 20%

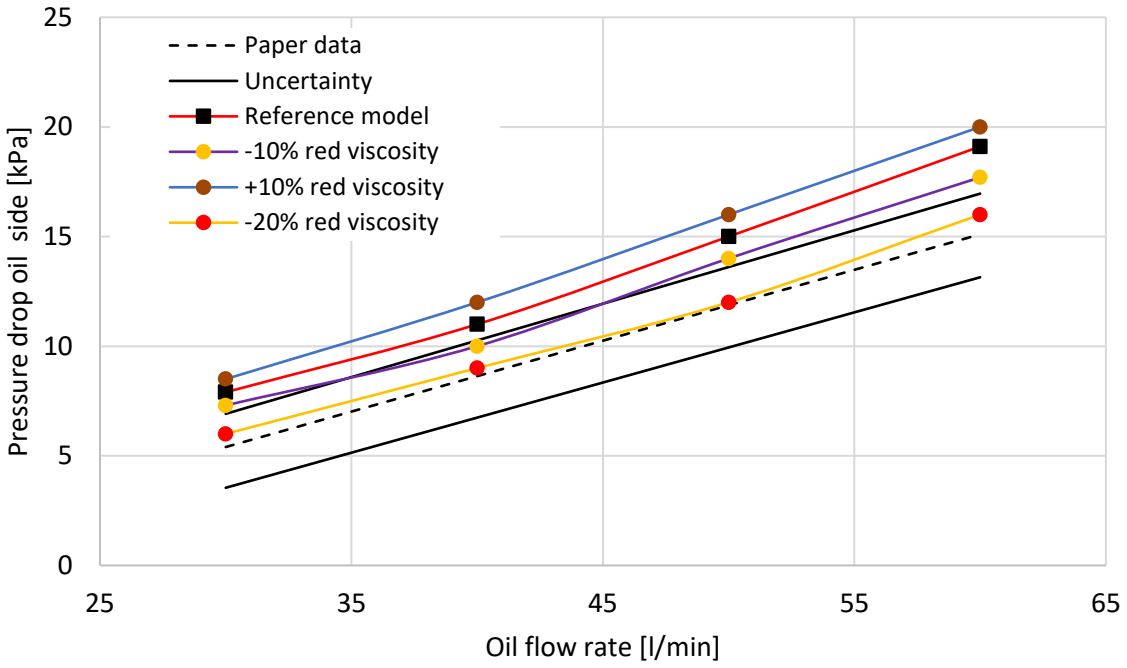


*Figure 50 - Oil pressure drop with air flow fixed at 560 std l/s – Geometry: Reference case – Different viscosity values*

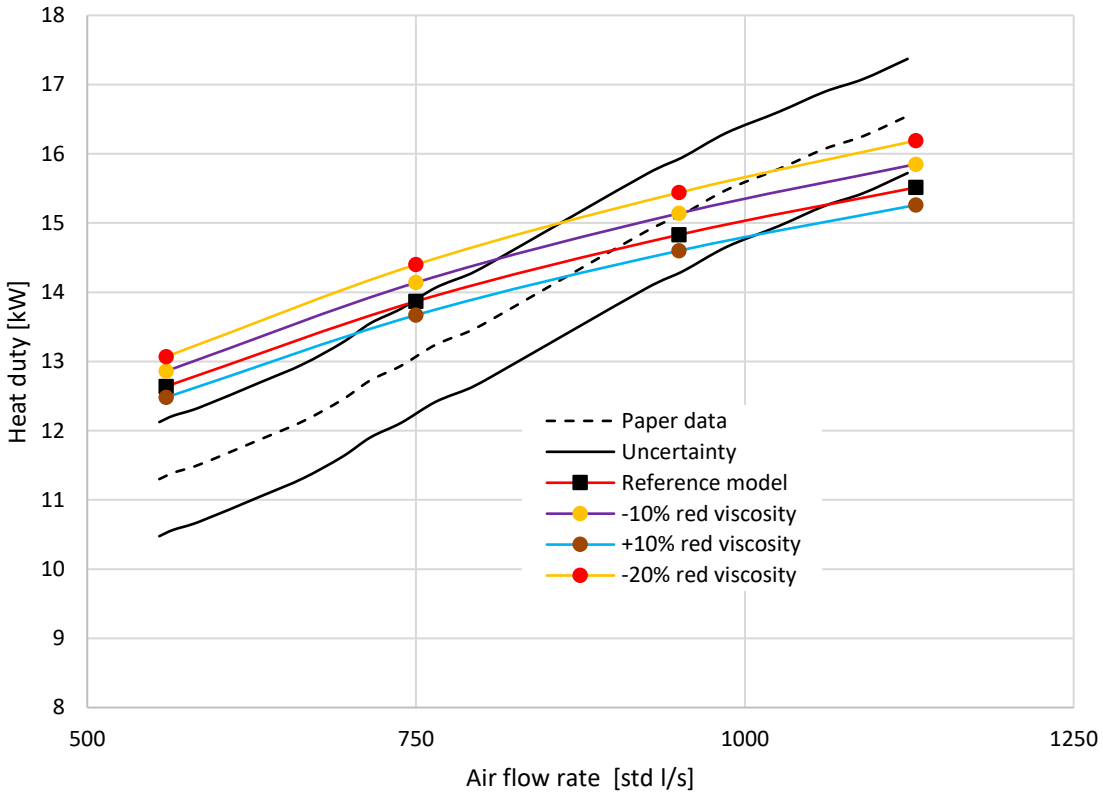


*Figure 51 – Heat duty with oil flow fixed at 60 l/min*

The chart shows that by only changing the viscosity (from +10% to -20%), the pressure drop and the Heat Duty have a maximum variation of 6%, in the design point.

After all these investigations, the main outcomes are that the sensitivity analyses of geometry and oil properties show that the model responds as expected to input changes, and all behavior observed are consistent and physically correct.

In order to investigate the reason for the pronounced underestimation of the heat duty visible in the Figure 35, an analysis of the HTC correlations used for this model has been conducted to identify any problems or inconsistencies in the thermal modeling.

## 5.4. Analysis on Air HTC

In order to quantify the underestimation observed on the reference case, a preliminary calculation has been performed. A preliminary analysis has been done to confirm that the air HTC is the main player in the variation of the thermal power trend. This preliminary analysis results are reported in Appendix B.

The Air HTC could be obtained starting from the equation of the Global Heat Transfer Coefficient *U,* defined in the paragraph 3.7, using the parameter UA calculated experimentally, the equations (46) and (47), and keeping all other parameters constant.

$$h_{air} = \frac{1}{UA} - h_{oil} - k_{metal} - f_{oil} - f_{air} \tag{46}$$

$$HTC_{air} = \frac{1}{h_{air} * LMTD_{corr} * \eta_{oil} * A_{wet,air}} \tag{47}$$

The Figure 52 shows the comparison between the air HTC calculated by the model and the value calculated using equation (47) as function of the air Reynolds number.

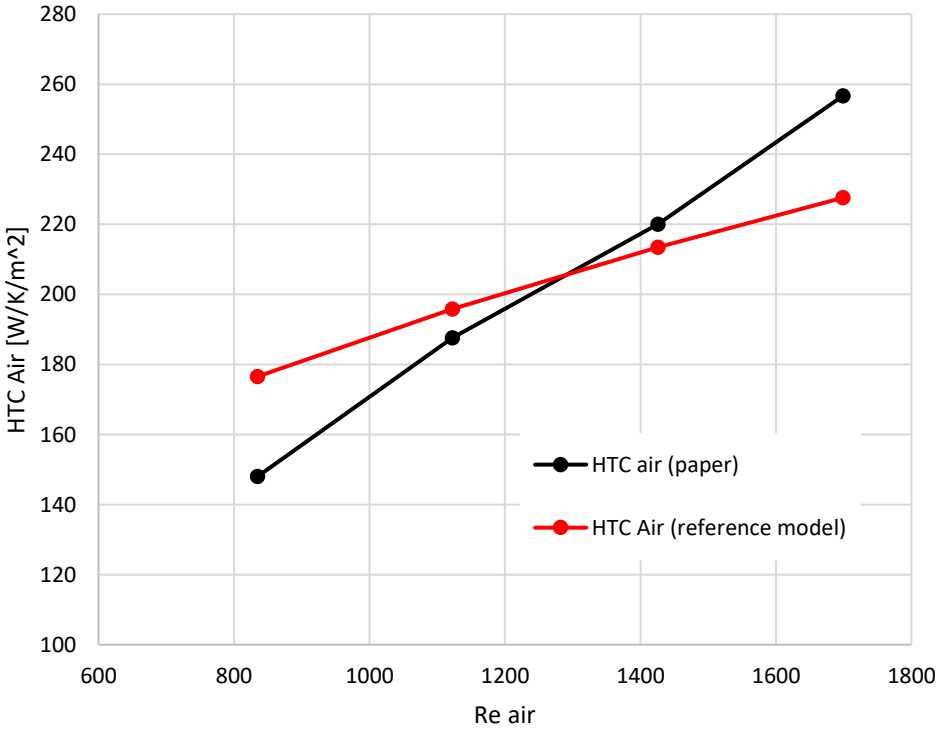


*Figure 52 – Air HTC trend as function of Air Re*

The two curves show a significantly different trend and, in analogy with what observed previously, it is clear that a new correlation is necessary to improve the model predictions.

A bibliographic research has been carry out to look for more correlations for air HTC calculation, applicable to the plate and fin heat exchangers. The research has these following objectives:

1. Check the compatibility of the selected correlation with other formulations from literature developed for similar Heat exchanger configurations
2. Verify in which cases the Heat Duty has a dependence from the air Re compatible with the one in the paper [8], i.e. an increase of 45% (from 11.5 kW to 16.5 kW) for Re numbers passing from approx. 835 to 1700 (equal to air flow from 560 std l/s to 1130 std l/s)
3. Check for literature correlations that are in better agreement with the experimental data

The more interesting correlations suitable for plate and fin heat exchanger have been implemented in the model. Using the geometry and all input related to the reference case a series of calculations has been performed to evaluate the impact of the air HTC correlation on the Heat Duty.

In the Figure 53 are summarized the results obtained with the different correlations to compare the heat duty trend as function of the air Re. The results of each case has been normalized using the heat duty obtained in the design point (with air flow equal to 560 l/s) for each correlation. With this normalization all trend lines start from 1 and shows the prediction error of each correlation as function of air Re.

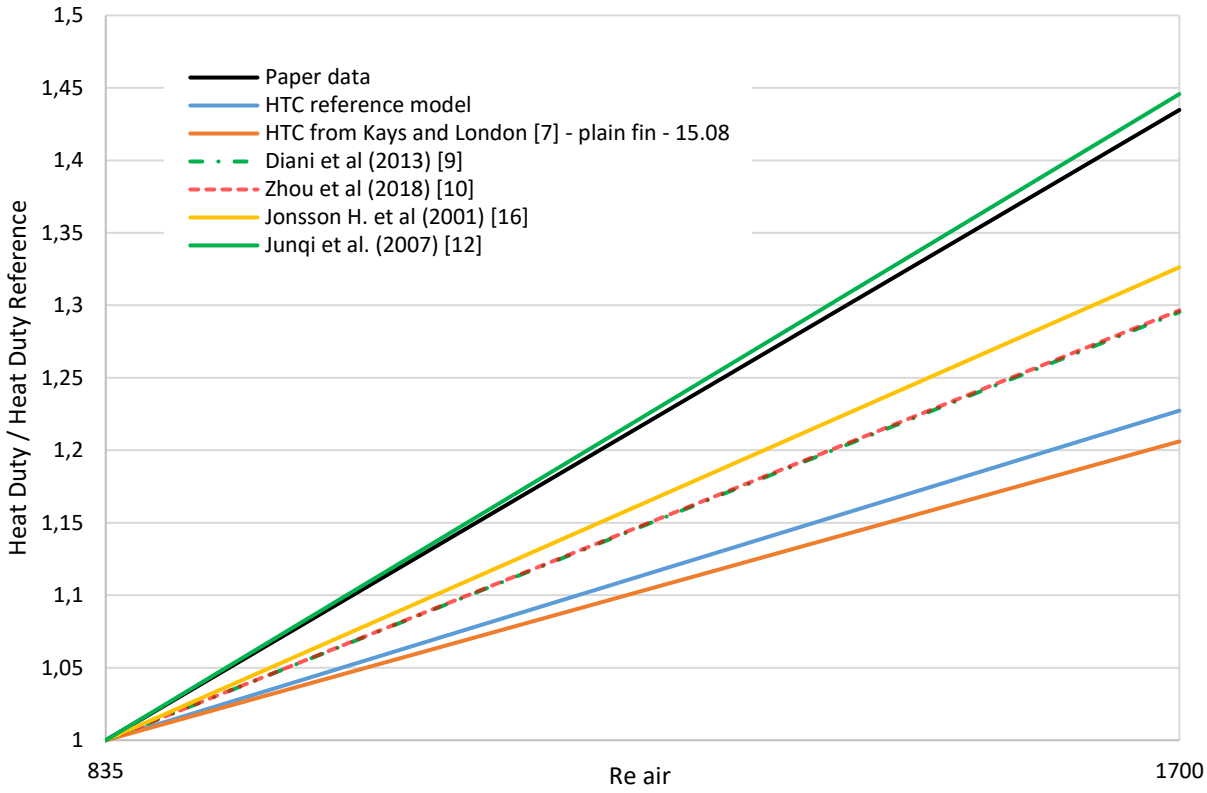


*Figure 53 – Plain and fin type - Dimensionless compare between different literature correlations for Air HTC calculation*

The plain and fin chart shows that:

i) the correlation selected for the reference model is comparable with all other literature correlations found

ii) the majority of the correlations implemented shows a less thermal power variation with air Re with respect to the data reported on the paper [8]

In order to evaluate a larger number of correlations the bibliographic research has been extended also for plain and tube exchangers, even if this type of exchanger are different respect to what presented in the paper [8].

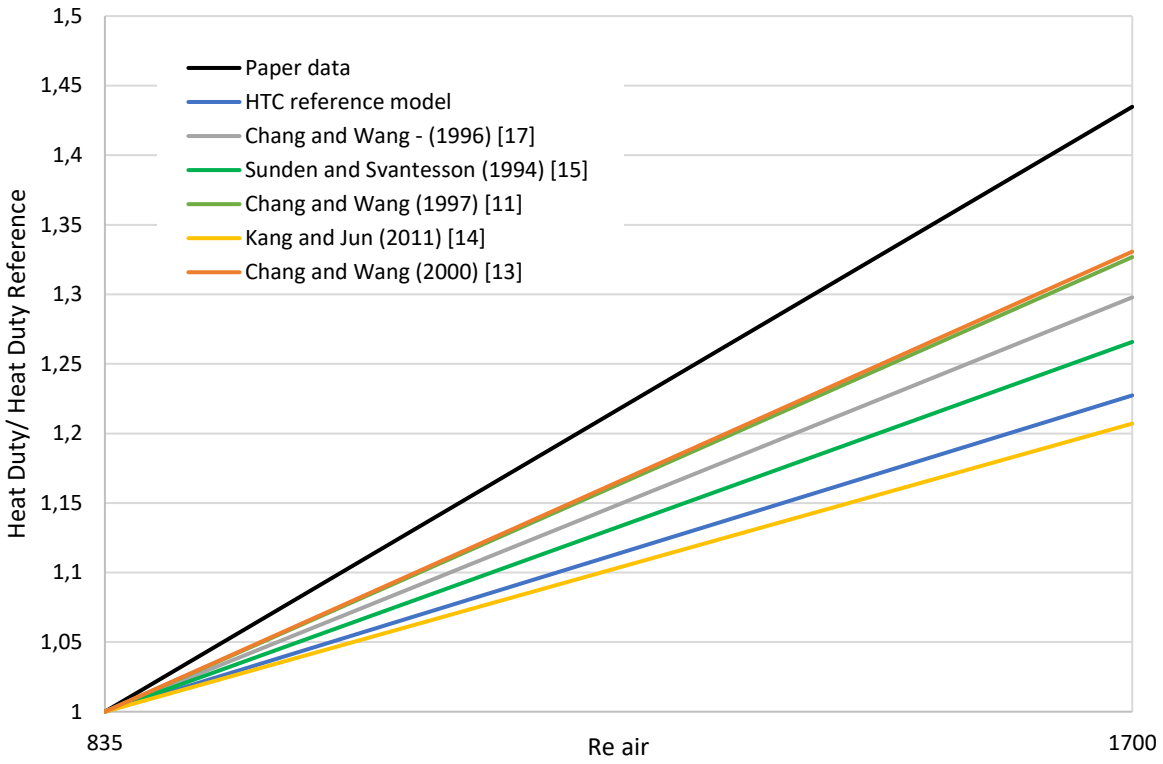


*Figure 54 – Plain and tube type - Dimensionless compare between different literature correlations for Air HTC calculation*

In Figure 54, the thermal power trends for the correlations applicable to plain and tube shows a global underestimation of Heat Duty respect to the experimental data. The maximum relative increase in Heat Duty is given by the correlation from Chang and Wang [11], which provides a Heat Duty increase approximately 30% against the 45% shown in the paper data.

Comparing all the results obtained from the survey, the formulation with the best match between predicted values and experimental data is the one described in the paper by Junqi et al. [12] (green line in the Figure 53), even though such correlation was initially built for heat exchangers with wavy fins.

The following graph will shows the results obtained with the new correlation for the estimation of the air HTC applied to the reference geometry with an oil flow equal to 60 l/min:

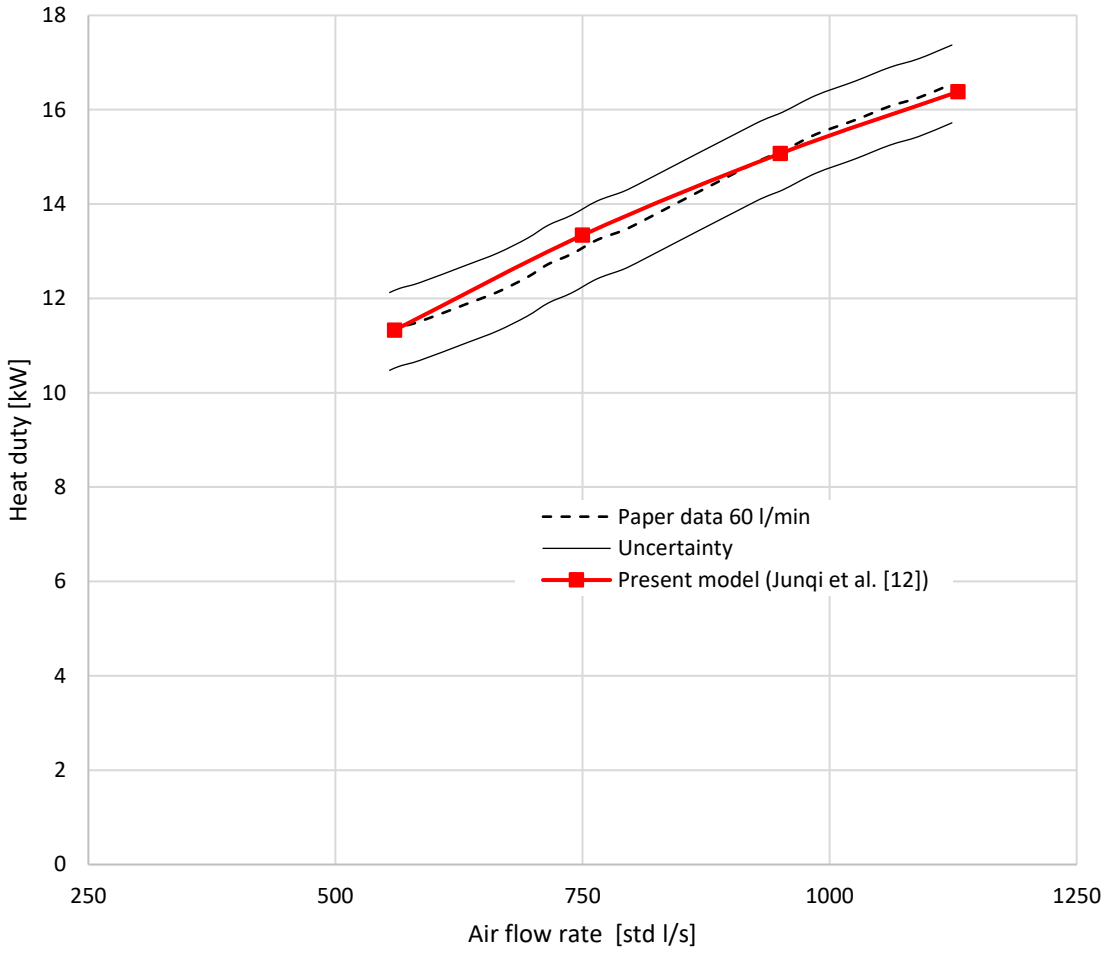


*Figure 55 – Heat duty for oil flow equal to 60 l/min with new correlation Air HTC*

In the Figure 55, the value of Heat Duty predicts from the model is very close to the experimental data, in particular, in the design point the value coincides exactly with the paper data. In general, the updated model with the new correlation shows an error lower than 3% respect to the experimental data and well below the experimental uncertainty.

The results for the 45 l/min and 30 l/min oil flow cases will be discussed in the following paragraph.

### 5.4.1. Notes on 45-30 l/min

Considering the good results obtained for the case with an oil flow of 60 l/min, the same model has been used with lower oil flow, 45 l/min and 30 l/min. As discussed in paragraph 5.1.2, these oil flow rates have low Reynolds numbers that are outside of the validity range of the oil HTC correlation implemented. The validity range cannot be displayed due to company intellectual propriety regulations.

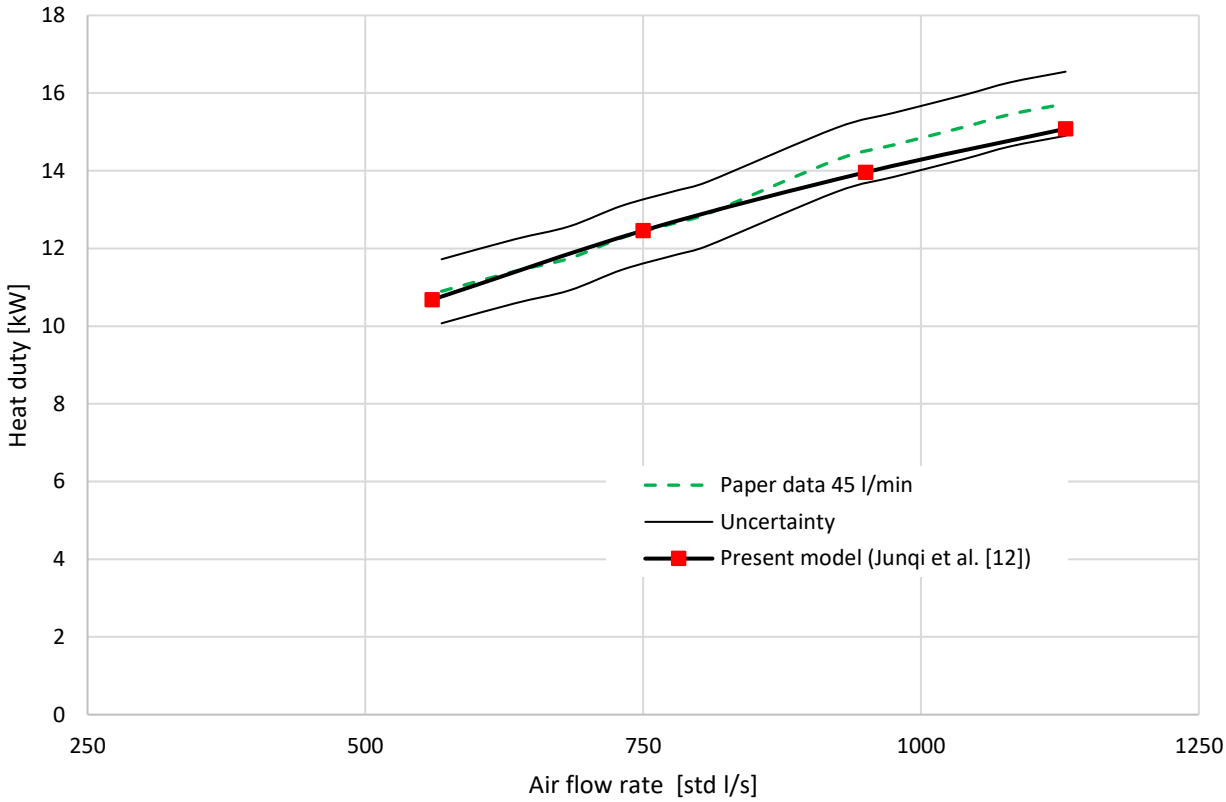


*Figure 56 – Heat duty for oil flow equal to 45 l/min with new correlation Air HTC*

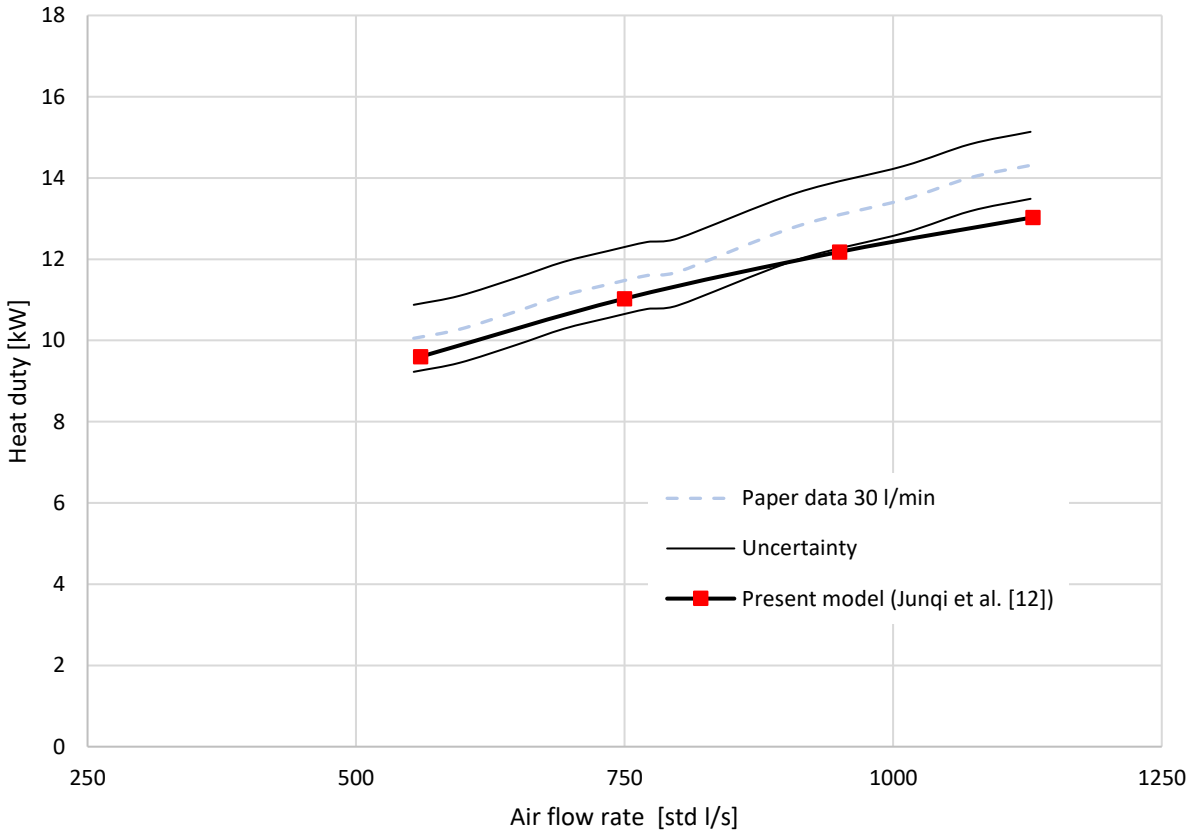


*Figure 57 – Heat duty for oil flow equal to 30 l/min with new correlation Air HTC*

In the Figure 56 and 57, the results predict by the model for the oil flow equal to 45 and 30 l/min are reported. The model provides a good agreement with paper data with respect to the reference case. The Heat Duty trend variation is well predicted but a relevant error at high air flow rate is present. The error could be attributed to the usage of the oil correlation out of range of validity that could affect the final results. To additional improve the model it will be necessary perform additional analysis to extend the actual correlation or identify new correlation more suitable for the cases under investigation.

# Chapter 6

# Validation with unpublished experimental data

After the validation of the model based on the public data available an additional validation phase has been performed using unpublished experimental data provided by the company.
The model predictions has been compared with three other experimental data sets taken on three different internal heat exchangers. The same sensitivity analyses were carried out and the accuracy of all HTC correlations shown was checked, in order to calibrate the model and develop a final, suitable HTC correlation for internal components using the literature study as starting point.
However, the results of these analyses cannot be disseminated and have been voluntarily omitted in this thesis (due to company intellectual propriety regulations).

# Chapter 7

# Conclusion

A ε-NTU method-based model was developed for the 0D design for plate and fin, counterflow, air – oil heat exchanger type. The model was validated using first the published experimental data available in the literature [8] and then with unpublished experimental data.
The comparison of the model prediction with published data [8] showed:

1. Good agreement with the air pressure drops (<30 Pa on all points) (Figure 39)
2. Good agreement with the oil pressure drops (<0.05 bar on all points) (Figure 40)
3. The error on Heat duty is +8% in design point and -6% at high air flow rate for the oil flow equal to 60 l/min (Figure 35 in paragraph 5.1.1)

In all the calculations carried out, a systematic underestimation of the Heat Duty with respect the experimental data was observed for high air mass flow rates. See the figures 35 and 52.
A sensitivity analyses were carried out on the following parameters:

i) Geometry
ii) Fluid properties
iii) Oil HTC correlations
iv) Air HTC correlations

to identify the one with a major impact on the model accuracy. Moreover, the results obtained from the survey was used to verify the correct response of the model to the different inputs.
The sensitivity analyses confirmed that the model works properly and that the first three parameters (see figures in the paragraphs 5.3.1 - 5.3.2 - 5.3.3 and Figure 58 in the Appendix B) have a low impact on the estimation of Heat Duty.

An in-depth literature research has been performed to identify more accurate correlations for air HTC estimation. The model has been updated with the correlation described by Junqi et al. [12].
The comparison with the published experimental data has been updated using the new predictions coming from the updated model. The chart in Figure 55 shows a very good agreement between the numerical model results and the literature experimental data, with an overall error less than 3%.

After this validation, the model was applied to additional three experimental data sets coming from a restricted company database, in order to develop a suitable HTC correlations (both air and oil) for internal components using the literature study as starting point [8]. All the details of the analysis on such test cases, as well as the final correlations adopted for both air and oil side, are voluntarily omitted from this thesis due to company intellectual propriety regulations.

# Chapter 8

# Recommendations and next steps

Starting from the work done, the next steps will be as follows:

1. Identify a new correlation suitable for very low oil Reynolds numbers (< 100) to improve the model accuracy for low oil flow, such as the cases with 45 l/min and 30 l/min.
2. Search additional published test cases in literature using different oil types in order to reduce uncertainties related to the formulation of oil properties.
3. Start a new research stream with focus on correlation for calculation of heat transfer coefficients for different fin heat exchanger configurations to increase the model flexibility.

# Appendix A

**Table of selected oil parameters**

- *SAE 10W-40*

| N° | Temperature | Density | Dynamic Viscosity | Specific Heat Capacity | Thermal Conductivity |
|---|---|---|---|---|---|
| | $[K]$ | $[kg/m^3]$ | $[Pa * s]$ | $[J/(kg * K)]$ | $[W/(m * K)]$ |
| 1 | 272.04 | 874.18 | 2.13E-01 | 1808.45 | 0.14 |
| 2 | 277.59 | 870.47 | 1.81E-01 | 1828.72 | 0.14 |
| 3 | 283.15 | 866.79 | 1.55E-01 | 1848.99 | 0.14 |
| 4 | 288.71 | 863.14 | 1.32E-01 | 1869.26 | 0.13 |
| 5 | 294.26 | 859.52 | 1.12E-01 | 1889.53 | 0.13 |
| 6 | 299.82 | 855.93 | 9.58E-02 | 1909.80 | 0.13 |
| 7 | 305.37 | 852.37 | 8.17E-02 | 1930.07 | 0.13 |
| 8 | 310.93 | 848.84 | 6.96E-02 | 1950.33 | 0.13 |
| 9 | 316.48 | 845.34 | 5.94E-02 | 1970.60 | 0.13 |
| 10 | 322.04 | 841.87 | 5.06E-02 | 1990.87 | 0.13 |
| 11 | 327.59 | 838.43 | 4.32E-02 | 2011.14 | 0.13 |
| 12 | 333.15 | 835.01 | 3.68E-02 | 2031.41 | 0.13 |
| 13 | 338.71 | 831.63 | 3.14E-02 | 2051.68 | 0.13 |
| 14 | 344.26 | 828.27 | 2.68E-02 | 2071.95 | 0.13 |
| 15 | 349.82 | 824.93 | 2.28E-02 | 2092.22 | 0.13 |
| 16 | 355.37 | 821.63 | 1.95E-02 | 2112.49 | 0.13 |
| 17 | 360.93 | 818.35 | 1.66E-02 | 2132.76 | 0.13 |
| 18 | 366.48 | 815.09 | 1.41E-02 | 2153.02 | 0.13 |
| 19 | 372.04 | 811.87 | 1.21E-02 | 2173.29 | 0.13 |
| 20 | 377.59 | 808.66 | 1.03E-02 | 2193.56 | 0.13 |
| 21 | 383.15 | 805.49 | 8.77E-03 | 2213.83 | 0.13 |
| 22 | 388.71 | 802.33 | 7.48E-03 | 2234.10 | 0.13 |
| 23 | 394.26 | 799.21 | 6.38E-03 | 2254.37 | 0.13 |
| 24 | 399.82 | 796.10 | 5.44E-03 | 2274.64 | 0.13 |
| 25 | 405.37 | 793.02 | 4.64E-03 | 2294.91 | 0.13 |
| 26 | 410.93 | 789.97 | 3.96E-03 | 2315.18 | 0.13 |
| 27 | 416.48 | 786.94 | 3.37E-03 | 2335.45 | 0.13 |
| 28 | 422.04 | 783.93 | 2.88E-03 | 2355.72 | 0.12 |

*Table 4 – SAE 10W-40 properties as function of temperature*

- *SAE 15W-40*

| N° | Temperature | Density | Viscosity dynamic | Specific Heat Capacity | Thermal Conductivity |
|---|---|---|---|---|---|
| | $[K]$ | $[kg/m^3]$ | $[Pa * s]$ | $[J/(kg * K)]$ | $[W/(m * K)]$ |
| 1 | 272.04 | 911.58 | 5.98E-01 | 1770.96 | 0.13 |
| 2 | 277.59 | 907.71 | 4.83E-01 | 1790.81 | 0.13 |
| 3 | 283.15 | 903.87 | 3.91E-01 | 1810.66 | 0.13 |
| 4 | 288.71 | 900.07 | 3.16E-01 | 1830.51 | 0.13 |
| 5 | 294.26 | 896.30 | 2.55E-01 | 1850.35 | 0.13 |
| 6 | 299.82 | 892.55 | 2.06E-01 | 1870.20 | 0.13 |
| 7 | 305.37 | 888.84 | 1.67E-01 | 1890.05 | 0.13 |
| 8 | 310.93 | 885.16 | 1.35E-01 | 1909.90 | 0.13 |
| 9 | 316.48 | 881.51 | 1.09E-01 | 1929.75 | 0.13 |
| 10 | 322.04 | 877.89 | 8.80E-02 | 1949.60 | 0.13 |
| 11 | 327.59 | 874.30 | 7.11E-02 | 1969.45 | 0.13 |
| 12 | 333.15 | 870.74 | 5.75E-02 | 1989.30 | 0.13 |
| 13 | 338.71 | 867.21 | 4.65E-02 | 2009.15 | 0.13 |
| 14 | 344.26 | 863.71 | 3.76E-02 | 2028.99 | 0.13 |
| 15 | 349.82 | 860.23 | 3.04E-02 | 2048.84 | 0.12 |
| 16 | 355.37 | 856.78 | 2.46E-02 | 2068.69 | 0.12 |
| 17 | 360.93 | 853.36 | 1.99E-02 | 2088.54 | 0.12 |
| 18 | 366.48 | 849.97 | 1.61E-02 | 2108.39 | 0.12 |
| 19 | 372.04 | 846.61 | 1.30E-02 | 2128.24 | 0.12 |
| 20 | 375.00 | 844.94 | 1.16E-02 | 2138.88 | 0.12 |
| 21 | 377.59 | 843.27 | 1.05E-02 | 2148.09 | 0.12 |
| 22 | 383.15 | 839.95 | 8.48E-03 | 2167.94 | 0.12 |
| 23 | 388.71 | 836.67 | 6.86E-03 | 2187.79 | 0.12 |
| 24 | 394.26 | 833.40 | 5.54E-03 | 2207.63 | 0.12 |
| 25 | 399.82 | 830.17 | 4.48E-03 | 2227.48 | 0.12 |
| 26 | 405.37 | 826.96 | 3.62E-03 | 2247.33 | 0.12 |
| 27 | 410.93 | 823.77 | 2.93E-03 | 2267.18 | 0.12 |
| 28 | 416.48 | 820.61 | 2.37E-03 | 2287.03 | 0.12 |
| 29 | 422.04 | 817.47 | 1.92E-03 | 2306.88 | 0.12 |

*Table 5 – SAE 15W-40 properties as function of temperature*

# Appendix B

- ***Additional confirmation on Air HTC***

To confirm that thermal power trend depends on the inappropriate correlations air HTC and not on the oil HTC, an additional analysis has been performed. First of all, the air HTC is the limiting factor in the calculation of the U parameter, therefore a variation of the oil HTC have to show no changes in the Heat Duty trend. To verify this assumption a variation study has been conducted increasing the value of oil HTC. The graph in the Figure 58 shows the trend of the dimensionless power (as it was done in the paragraph 5.4) as a function of the air Reynolds number in 4 different cases:

i) Paper data
ii) Reference model
iii) Reference model with the value of oil HTC increase of 20%
iv) Reference model with the value of oil HTC infinite (ideal case). In this case, the thermal exchange will depend only on the air HTC (the other thermal resistances are negligible compared to the latter)

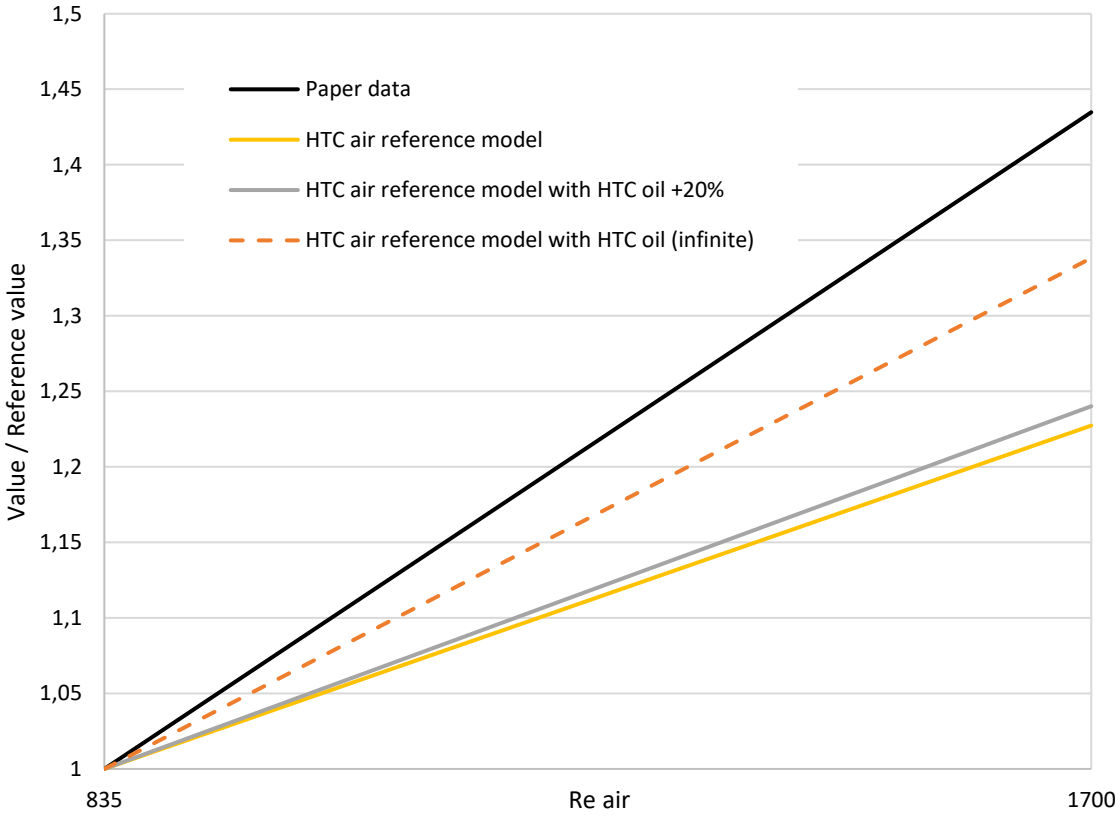


*Figure 58 – Dimensionless compare between Air HTC of two chosen correlation with paper data [8]. The dash line indicates that HTC oil is infinite*

Considering the best case (ideal case with oil HTC infinite), the correlation used up to now does not provide the same trend of the paper experimental data. This result confirms that the model prediction uncertainties are related to correlation expression selected for the calculation of air HTC.

# Bibliography

[1] Incropera, DeWitt, Bergman and Lavine, Fundamentals of Heat and Mass Transfer, Sixth Edition.

[2] F. A. Mota, E. Carvalho and M. A. Ravagnani, "Modeling and design of plate heat exchanger," *Intech,* July 2015.

[3] M. Picon-Nuñez, G. Polley, E. Torres-Reyes and A. Gallegos-Muñoz, "Surface selection and design of plate-fin heat exchangers," *Applied Thermal Engineering,* pp. 917-931, 1999.

[4] H. E. Ahmed, H. A. Mohammed and M. Z. Yusoff, "Heat transfer enhancement of laminar nanofluids flow in a triangular duct using vortex generator," *Superlattices and Microstructures ,* vol. 52, pp. 398-415, 2012.

[5] R. M. Manglik and A. E. Bergles, "Heat Transfer and Pressure Drop Correlations for the Rectangular Offset Strip Fin Compact Heat Exchanger," *Experimental Thermal and Fluid Science ,* pp. 171-180, 1995.

[6] R. K. Shah and D. P. Sekulic, Fundamentals of heat exchanger design, John Wiley & Sons, Inc, 2003.

[7] W. M. Kays and A. L. London, Compact Heat Exchangers, 3rd Ed., 1984.

[8] B. J. Hathaway, K. Garde, S. C. Mantell and J. H. Davidson, "Design and characterization of an additive manufactured hydraulic oil cooler," *International Journal of Heat and Mass Transfer,* no. 117, pp. 188-200, 2018.

[9] A. Diani , S. Mancin, C. Zilio and L. Rossetto, "An assessment on air forced convection on extended surface: Experimental results and numerical modeling," *International Journal of Thermal Sciences,* no. 67, pp. 120-134, 2013.

[10] G. Zhou, Y. Ye, J. Wang, W. Zuo, Y. Fu and X. Zhou, "Modeling air-to-air plate-fin heat exchanger without dehumidification," *Applied Thermal Engineering,* pp. 137-148, 2018.

[11] Y.-J. Chang and C.-C. Wang , "A generalized heat transfer correlation for louver fin geometry," *International Journal Heat Mass Transfer,* vol. 40, pp. 533-544, 1997.

[12] D. Junqi, C. Jiangping, C. Zhijiu, Z. Yimin and Z. Wenfeng, "Heat transfer and pressure drop correlations for the wavy fin and flat tube heat exchangers," *Applied Thermal Engineering,* no. 27, pp. 2006-2073, 2007.

[13] C.-C. Wang, K.-Y. Chi and C.-J. Chang, "Heat transfer and friction characteristics of plain fin-and-tube heat exchangers, part II: Correlation," *International Journal of Heat and Mass Transfer ,* no. 43, pp. 2693-2700, 2000.

[14] H. C. Kang and G. W. Jun, "Heat transfer and flow resistance characteristcs of louver fin geometry for automobile applications," *Journal of Heat Transfer ,* vol. 133, 2011.

[15] B. Sunden and J. Svantesson, "Correlation of j- and f-factors for multilouvered heat transfer surfaces," *Proceeding of the 3rd UK National Heat transfer Conf.,* pp. 805-811, 1992.

[16] H. Jonsson and B. Moshfegh, "Modeling of the thermal and hydraulic performance of plate fin, strip fin and pin fin heat sinks-influence of flow bypass.," *IEEE Trans. Compon. Packag. Technol. ,* no. 24, pp. 142-149, 2001.

[17] Y. J. Chang and C. C. Wang, "Air side performance of brazed aluminium heat exchangers," *Journal Enhanced Heat Transfer,* vol. 3, pp. 15-28, 1996.